Deep Sea Research Part I: Oceanographic Research Papers
February 2021, Volume 168, Pages 103449 (15p.)
https://doi.org/10.1016/j.dsr.2020.103449
https://archimer.ifremer.fr/doc/00660/77182/

A local scale analysis of manganese nodules influence on the Clarion-Clipperton Fracture Zone macrobenthos

Francesca Pasotti [1, *], Mevenkamp Lisa [1], Pape Ellen [1], Błażewicz Magdalena [3], Bonifácio Paulo [4], Riehl Torben [5], De Smet Bart [2], Lefaible Nene [1], Lins Lidia [1], Vanreusel Ann [1]

[1] Marine Biology Laboratory, Ghent University, Ghent, Belgium
[2] Flanders Marine Institute, Oostende, Belgium
[3] Department of Polar Biology and Oceanobiology, University of Łódź, Łódź, Poland
[4] Ifremer, Centre Bretagne, REM EEP, Laboratoire Environnement Profond, ZI de la Pointe du 5 Diable, CS 10070, F-29280, Plouzan, France
[5] Biocenter Grindel & Zoological Museum, University of Hamburg, Hamburg, Germany

* Corresponding author : Pasotti Francesca, email address : francesca.pasotti@ugent.be

Abstract :

The present investigation focuses on the Global Sea Mineral Resources contract area B4S03 site in the Clarion-Clipperton Fracture Zone nodule fields. We investigated the sedimentary characteristics and the higher-taxon (order/class) and lower-taxon (family, morphospecies) diversity of the soft sediment macrobenthos with special focus on the dominant taxa (Isopoda, Polychaeta, Tanaidacea) in relation to nodule abundance. Across all analyses no consistent and/or significant differences between the two nodule-rich and the nodule free stations were found in terms of abiotic or biotic factors, suggesting that both habitat-types have similar sedimentary conditions and that macrofauna is represented by comparable densities and higher-taxon diversity across stations. Rarefaction/accumulation curves and sample coverage analysis shows that the current sampling effort was insufficient to characterize the B4S03 site diversity at morphospecies level but covered >90% of the diversity at the family level for the three dominant taxa. The high number of singletons encountered, the patchiness and low densities of the investigated taxa coupled to the logistically limited potential for replication per habitat/station, may point to under-sampling bias of the current study with the risk to underestimate species diversity and overestimate endemism. We recommend a more extensive sampling with the combination of molecular tools coupled with taxonomical expertise.

Highlights

► GSR B4S03 nodule-rich and nodule-free stations are characterized by similar sedimentary parameters. ► The nodule-rich stations showed comparable macrofauna densities but higher-taxon diversity to that of the nodule-free station. ► The sampling effort was insufficient to characterize the dominant taxa's diversity at morphospecies level. ► When the family level is considered >90% of the diversity was sampled during this study. ► The high number of singletons, the patchiness and low densities may lead to an underestimation of species diversity. ► The high number of singletons, the patchiness and low densities may lead to an overestimation of endemism.

1 Introduction

Recent studies indicated that significant metals and rare earth elements resources - needed for the manufacturing of increasing numbers of high-tech products and green technologies for decarbonisation - are stored at the bottom of the oceans in the form of deep-sea mud and ferromanganese crusts, whereas rare metals (e.g., nickel, copper, cobalt and manganese) are found in polymetallic nodules (Burns and Burns, 1977; Petersen *et al.*, 2016; Balaram, 2019). Polymetallic nodules were first discovered in the Kara Sea (Arctic Ocean) during the Challenger expedition in 1870 (Murray and Renard, 1891). These nodules form at depths ranging from 4000 to 6000 m on the oceans' abyssal plains through processes of mineral precipitation over millions of years. The Clarion-Clipperton Fracture Zone (CCFZ) extends for 6 million km^2 in between the Clarion and Clipperton fractures, off the west coast of Mexico in the North-East Pacific. This region has been estimated to be the largest deep-sea polymetallic nodule reserve in the world (Peterson et al., 2016) and it has been since 1997 at the centre of the International Seabed Authority (United Nations) plans of work for exploration.

The deep sea harbours some of the most understudied ecosystems of our Planet where organisms have adapted to particular environmental conditions such as high pressure and low food availability (Smith et al., 2017). Renowned for its high biodiversity and low densities (Glover and Smith, 2003; Smith *et al.*, 2008a; Rex and Etter, 2010), the deep sea hosts a large number of undescribed species (Bonifácio and Menot, 2019) as well as phylogenetic lineages represented nowhere else (Riehl *et al.*, 2014; Christodoulou *et al.*, 2019), and nodule fields are no exception (Amon *et al.*, 2016; Bonifácio and Menot, 2019; Błażewicz *et al.*, 2019; Gheerardyn and George, 2019; Jakiel *et al.*, 2019; Wiklund *et al.*, 2019). Since the 1970s an increasing number of expeditions took place with the common goal to estimate the biodiversity of the CCFZ nodule fields' macrobenthic communities. These investigations reported a generally unanticipated high and clearly under-sampled biodiversity which appeared to be directly related to the taxa abundance (the higher the abundance, the higher the diversity of a taxon) and its relationship to the longitudinal surface water productivity gradient in the area (Smith *et al.*, 1996, 1997; Smith and Demopoulos, 2003; Smith *et al.*, 2008a; Amon *et al.*, 2016, 2017; Dover *et al.*, 2017; Bonifácio and Menot, 2019). Further, other studies have indicated that the presence of polymetallic nodules on otherwise "de-

sert-like" abyssal landscapes, influences the diversity, composition, distribution and abundance of meio-, macro- and megafauna in the region (Veillette *et al.*, 2007a; Smith *et al.*, 2008a; Amon *et al.*, 2016; Vanreusel *et al.*, 2016; De Smet *et al.*, 2017). The surface of the nodules may act as anchorage substrate for sessile filter feeder species (such as alcyonaceans and antipatharian corals), thousand-years-old glass sponges and the associated interspecies assemblages (e.g. ophiuroids living on stalked sponges) which are otherwise virtually absent in the surrounding nodule-void sediments (Vanreusel *et al.*, 2016; Kersken *et al.*, 2019). Veillette *et al.*, (2007a, 2007b) found that both at a regional and at the nodule facies scale, the texture and the extent of the exposed surface of these ferromanganese accretions displayed a structuring effect on the distribution and diversity of encrusting Foraminifera. Finally, the internal structure of the nodules seems to host specific crevice fauna, which differs in diversity and composition from that found outside the nodules (Pape *et al.*, In prep.; Bussau, 1993; Thiel *et al.*, 1993; Maybury, 1996; Veillette *et al.*, 2007b, 2007a) Depending on management practices applied both during and after the nodule harvesting process, these functional groups may be lost from the exploited area without viable routes and substrates for recolonization.

The present analysis focuses on the soft sediment macrobenthos of the Global Sea Mineral Resources (GSR, Belgium) contract area and aims at providing new baseline information on the local-scale diversity patterns of soft sediment macrobenthic communities in relation to nodule abundance. We investigated the higher-taxon (order/class) macrofaunal assemblage structure and the lower-taxon (family, morphospecies) diversity of the three most abundant taxa (Isopoda, Polychaeta, Tanaidacea) by comparing two nodule-rich and one nodule-free habitat within one site (B4S03) in the GSR contract area. Furthermore, we present a list of identified morphospecies belonging to the three most dominant taxa and provide an estimation of the sampling effort necessary to observe different proportions of the estimated asymptotic diversity for the investigated B4S03 site. We hypothesize that the two nodule-rich stations investigated within this study will be similar in terms of higher-taxon and main taxa species/family composition of the whole assemblage, while differing from the nodule-free station. We also hypothesize a higher heterogeneity in environmental characteristics at the two nodule-rich stations with overall no differences in sedimentary feature among the three stations. Due to the local scale of this study (stations are located within a range of 2-10 km) and building on the relationship between benthic abundances and the regional

trends in the eupohotic zone productivity (Smith et al., 2008), we, moreover, do not expect differences in the total macrobenthic abundances between the three investigated stations.

2 Material and Methods

2.1 Study area and sampling design

The GSR contract area is comprised of three separate zones (B2, B6 and B4; Figure 1) located along a west to east direction within the CCFZ in the North-East Pacific Ocean. Based on the spatial heterogeneity in hydrodynamic features ultimately controlling primary productivity in the oceanic Eastern-Tropical Pacific, Pennington *et al.* (2006) delineated seven biogeographical provinces. Most of the GSR concession area falls within the North Equatorial Current (NEC) province (13-23° N, 110/115 – 140°W). Within zone B4, the site B4S03 (10 x 20 km) is located in between 14.13°N - 14.0 °N and 125.95° W - 125.85° W. As part of the commitment of GSR to follow the International Seabed Authority Recommendations (ISBA/25/LTC/6) provided for the Environmental Impact Assessment of future mining activities in the contract areas, we identified within the GSR B4S03 site a group of stations with high abundance of nodules and one site which is virtually nodule-free to investigate the soft sediment macrobenthic assemblages.

This study is based on samples collected during the GSRNOD17 expedition, which took place on board of the RV 'Topaz Captain' during May-June 2017. During the cruise two nodule-rich (Nodrich_A and Nodrich_B) and one nodule-free (Nodfree) stations were sampled (Figure 1). Nodule presence/absence at the sampling sites was established by means of multibeam echosounder (MBES) backscatter intensity data and AUV seabed photographs gathered during the preceding GSR cruise (GSRNOD15A; Pape *et al.*, 2016; Juan *et al.*, 2018) and verified by nodule abundance data from box-corer samples. Nodrich_B and Nodfree stations were located within an area of about 5 x 5 km in the south-west of the B4S03, with Nodfree situated 2.6 km north from Nodrich_B. Nodrich_A was located in the north-east of B4S03 at a distance of about 7-10 km from the southern stations (see map in Figure 1). Within each station, a series of multiple-corer (MUC, MC-800 series Ocean instruments, Inc.) and box-corer (BC, model BX-650, Ocean Instruments, Inc.) deployments were performed to sample the sediment environmental parameters (MUC) and to collect the macrofauna (BC, see supplementary table ST1). To cover the spatial heterogeneity of the area, the deployments were conducted a few hundreds of meters apart from each other (see location of BC on map Figure 1). All stations had a depth range of 4480-4649 m and nodule presence/absence was considered to be the main factor determining most of the differences between the three sampling stations.

2.2 Sampling strategy and sample processing

2.2.1 Abiotic variables

The environmental differences between the three stations were estimated from a total of eleven MUC (sediment biogeochemistry: four at a Nodfree station, four at the nodule-rich station Nodrich_B and three at Nodrich_A; supplementary table ST1). Upon recovery, the cores (PVC cores of 10 cm diameter) removed from the MUC were transferred to a cold lab container set at a temperature of +4°C. Before processing, the cores were examined for the presence of nodules. The sediment was sliced per 1 cm layer till a depth of 10 cm and storage was specific for the type of analysis: pigments (Chlorophyll-a and Phaeopigments) at -80°C; total organic carbon (TOC), total nitrogen (TN) and grain size at -20°C. Each sediment slice for the analyses of grain size, TOC and TN was dried at 60°C overnight in the laboratory in Ghent, Belgium. After drying, 1 g of sediment was analysed with a Malvern Mastersizer Hydro 2000 G for granulometry. The granulometric parameters used within this study are median grain size (Median_gs), sorting coefficient (Grain_SC), sand (grain size > 63 µm), silt (4 µm < grain size < 63 µm), and clay (grain size < 4 µm) content (%) as well as porosity (% vol.). The sorting of the sediment as a measure of the spread of the various grain size classes, was quantified by the sediment sorting coefficient (Grain_SC), calculated following Giere (2009) as:

$$SC = \frac{\varphi 2s - \varphi 7s}{2}$$

With ϕ2s and ϕ7s being the logarithm (base 2) of the first and third quartile of the sediment grain size frequency distribution. The higher the value of Grain_SC, the less well sorted the sediment is and the more it is represented by one grain size class. Porosity (ϕ) was estimated assuming a dry sediment density of 2.55 g cm^{-3} and making use of the formula:

$$\varphi = \frac{\frac{weight\ of\ water}{density\ of\ water}}{\frac{weight\ of\ dry\ sediment + weight\ of\ water}{density\ of\ water}}$$

Total organic carbon (TOC) and total nitrogen (TN) were measured on samples of 200 mg using a Flash 2000 NC Sediment Analyser of Interscience (Thermo scientific). These samples were acidified with 1% HCl to remove inorganic carbon prior to analysis. The (molar) sediment total organic carbon to total nitrogen ratio (TOC/TN) was computed as:

$$\frac{TOC}{TN} = \frac{\frac{TOC}{12}}{\frac{TN}{14}}$$

Pigment analysis was carried out for each 1 cm layer on the 0-5 cm layer profile by means of High Performance Liquid Chromatography (Agilent 1200 Infinity II, Agilent Technologies, Diegem, Belgium). Chlorophyll-a and its breakdown product phaeophytin-a were measured and their sum as chloroplastic pigments equivalent (CPE) calculated. Nodule coverage was calculated on eleven box-corers deployments that were retrieved for the macrofauna sampling (see next section for more details). The nodule abundance and coverage was calculated by GSR staff with two methods: i) from each individual box-corer each nodule was weighed and the sum of the weights was divided by the box-corer surface (0.25 m^2); ii) for AUV imagery the surface was estimated as the percentage of the total box-corer surface occupied by the nodules based on photographs taken after the overlying water was siphoned out of the newly retrieved box-corer on deck (see next section on macrofauna assemblage sample processing for more details).

2.2.2 Macrofauna assemblage

For the sampling of the macrobenthic fauna, a point-sampler stainless steel box-corer (BC, 0.5 length x 0.5 m width, 0.6 cm height) was used. Four box-corer deployments were successfully conducted at Nodfree and Nodrich_B, whereas only three box-corer deployments were successful at Nodrich_A. For each box-corer deployment a MUC sample was taken at the same location (supplementary table ST1), allowing for inference on the possible relationships between the community composition and the local environmental variables. Upon retrieval, the sediment-overlying water was removed from the box-corer and filtered upon a 300 µm sieve to retain all possible macrofauna organisms present in the overlying water. Once the water and surficial nodules were removed, the sediment within the box-corer was sliced in 0-3 cm, 3-5 and 5-10 cm layers by means of a ruler and spatulas. The sediment collected by slicing, was

162 transported submerged in cold filtered sea water into a climate room set at +4°C to be live sieved (300
163 µm). The sieved macrofauna was collected and fixed in prechilled non-denatured 96% EtOH (-20°C) for
164 further identification (to the lowest taxonomic level possible), which was done in the laboratory back in
165 Belgium. Identification was carried out on ice and in pre-filtered seawater (on board) or Milli-Q water
166 (later in the laboratory) to avoid DNA degradation for further DNA barcoding (results not discussed
167 here). Identification to species level was done only for the most abundant taxa: Isopoda, Polychaeta,
168 Tanaidacea. When the identification of intact specimens to species/family level was not possible with
169 absolute certainty, the most closely resembling species/family was chosen and a "cf." annotation was
170 mentioned next to the species name. The identification of intact specimens was done by expert taxono-
171 mists (co-authors of this paper, see Contribution section) using identification keys and original taxonom-
172 ic descriptions. Total counts per box-corer were extrapolated to densities (number of individuals per
173 square meter, ind. m^{-2}) to allow comparison with other studies. The higher-taxon processing included
174 the counting of macrofauna-size meiofaunal taxa (total counts are reported in the supplementary Table
175 ST2) but it was decided not to include these data in the analyses for comparability with other studies.

176 *2.2.3 Data and Statistical Analysis*

177 One of the interests of this paper was to identify possible differences in environmental variables,
178 community composition and higher/lower-taxon diversity between nodule-rich and nodule-free stations.
179 Since the replication of a nodule-free station was not possible (only one nodule-free station was
180 sampled) during the GSRNOD17 cruise, the analysis of the collected data was carried out considering all
181 the stations separately (factor "Station"= 3 levels: Nodfree, Nodrich_A, Nodrich_B). All statistical analyses
182 results are reported in Table 1 a and b (main test) and in supplementary material Table ST3 a and b
183 (pair-wise comparisons). All analyses were performed in R with the use of the RStudio interface (version
184 1.2.1335, R Core Team, 2020). Both the univariate (e.g. nodule abundance, individual sediment
185 characteristics/individual pigment concentrations, total density, main taxa relative abundance, and
186 diversity indices) and the multivariate (e.g. all environmental variables excl. nodule abundance / higher-
187 taxon abundances) datasets were tested for differences by means of a One-way (only factor : Station) or
188 Two-way (with as factors: Station, Layer and their interaction) Permutational Multivariate Analysis of

Variance (Permanova). The analysis were computed based on a Euclidean distance dissimilarity matrix for all the univariate datasets (raw data) and the environmental variable multivariate dataset (normalised raw data), whereas a Bray-Curtis similarity matrix was calculated for the higher-taxon multivariate dataset on square-root transformed density data (ind. m-2). Where a significant effect was found, PermDisp analysis was done to confirm homogeneity of dispersions between groups and interpret the Permanova results. If significance was confirmed, a pair-wise test was carried out to identify the stations that differed from one another. The analyses were executed making use of the following R packages: "vegan" (for the Permanova analysis, version 2.5.5, Oksanen *et al.*, 2019), "RVAideMemoire" (for MANOVA pair-wise testing, version 0.9-73, Hervé, 2020), "stats" (for the post hoc t-test, version 3.6.1, R Core Team, 2020), "ecodist" (for dissimilarity based functions, version 2.0.1, Goslee and Urban, 2020), "fossil" (for Chao1 asymptotic diversity estimator, version 0.3.7, Vavrek, 2020) and "iNext" (Interpolation and Extrapolation of Species Diversity, version 2.0.19, Hsieh and Chao, 2019). To visualise the number of unique and shared species and families per taxon as a set of intersections between the three stations, we used the upset() function in the "UpSetR" package (version 1.4.0, Gehlenborg, 2019). In the iNext package, the Authors make use of Hill numbers for abundance data to estimate the asymptotic diversity. In our study we used for this estimation q = 0 (for more details see ; Hsieh et al., 2016) which equals to the simple species (taxon) richness, which counts species regardless of their relative abundance (Chao et al., 2014).

2.2.3.1 Abiotic variables analysis

A multivariate two-way permanova was carried out on the 0-5 cm and 5-10 cm profiles for all variables (excl. nodule abundance), with pigments being absent for the deeper 5-10 cm layer. The univariate statistical analyses pertaining to the pigments were carried out separately from the other environmental variables since the data was analysed across a higher resolution sediment profiling and reported as such to avoid loss of information during analysis. Differences in individual pigment concentrations (Chl-a, Phaeopigments, CPE) between stations were analysed across five surface sediment layers (0-1, 1-2, 2-3, 3-4, 4-5 cm) whereas the other environmental variables (granulometry, TOC, TN) were analysed for the two bulk depth profiles 0-5 and 5-10 cm. To visualise the sediment environmental data a Principal Coordinate Analysis (PCA) was built on a Euclidean distance-base dissimilarity matrix of the complete dataset

216 (including the pigments - as bulk 0-5 cm - but excl. nodule abundance) normalised data (Figure 2) and
217 group confidence interval (0.95) ellipses were constructed. Average values (with standard deviation) of
218 the investigated parameters are reported in Table 2. For completeness, we provide two PCA plots for the
219 0-5 and 5-10 cm depth profile for the sole sediment abiotic variables (without the pigments and nodule
220 abundance) in the supplementary material Figure SF1 and SF2.

221 To have a proxy for surface water productivity we extracted VGPM (Vertically Generalized Production
222 Model) based on MODIS satellite data for January 2015 - June 2017 (1080 x 2160 files) and estimated
223 net primary productivity (NPP, Figure 3; Behrenfeld and Falkowski, 1997). In order to account for time-
224 lagged responses in faunal and abiotic characteristics (Miljutin *et al.*, 2015), we set the start of the
225 estimation period to nine months prior to the GSRNOD15A sampling campaign. Monthly-averaged NPP
226 values were downloaded as HDF files (http://www.science.oregonstate.edu/ocean.productivity/index.php),
227 converted to geotiff (using SeaDAS) and finally perfected in QGIS v2.18 when a convex hull was drawn
228 around the positions of all biological deployments and the Zonal statistics tool was used to compute
229 monthly averaged NPP.

230 *2.2.3.2 Macrofauna higher-taxon analysis*

231 Because of the low densities, the macrofauna higher-taxon assemblage was analysed in bulk merging
232 the 0-3, 3–5 cm and 5-10 cm layer (hence as bulk 0-10 cm). All results of univariate and multivariate
233 analyses are reported in Table 1 b and ST3 b.

234 *2.2.3.3 Diversity analysis*

235 To compare species/family diversity for each of the three dominant taxa and higher phylum/order level
236 for the macrofauna higher-taxon dataset, we carried out multiple One-way Permanova on the estimated
237 diversity indices for each taxon separately (Table 1 b). For this study we selected i) the species/taxon
238 richness number (S or T), ii) the Shannon - Wiener index (H') iii) The Pielou's evenness index and iv) the
239 rarefaction method of Sanders (1968), perfectioned by Hurlbert (1971), of expected species (ES(n)) for a
240 specific sample size (smaller or equal to the effective n= minimum taxon number; for average values see
241 Table 3).

To visually portray the distribution of species and families between stations (shared versus unique species/families) we produced three plots (one per taxon, Figure 4 a-c) each displaying both the species and the family shared/unique counts across the three sites. A list of unique (found only at one specific station across all samples) and singleton (encountered only once across all samples) species is given in the supplementary material Table ST4. Finally, a plot with the average relative abundance of the families per taxon per station and for the whole B4S03 site is presented in Figure 5.

2.2.3.4 Asymptotic diversity analysis (low taxonomic level)

To understand the efficiency of our sampling effort in capturing the local diversity (B4S03 site) for the three most dominant taxa, we used the R package "*fossil*" to compute for both species and family level the non-parametric asymptotic richness estimator Chao1 (see Table 4). In this study we focused our analysis on the Chao1 estimator which is a widely used non-parametric estimator of species richness for abundance data which takes into consideration the number of singletons (number of species represented by one singular individual across samples) and doubletons (species represented by two individuals across samples) in the data matrix (Chao *et al.*, 2009). To estimate the minimum number of additional individuals/samples or sampling area necessary to detect different proportions (with g = 1 representing 100% of the estimated diversity) of the estimated S_{Chao1} asymptotic richness for the whole B4S03 site we made use of the Excel Calculator for abundance data (using total counts) as provided in the Appendix by Chao et al. (2009). To visually display the standardised species richness estimation and the sample coverage based on the Hill's numbers (in our case we used *q=0* which gives the familiar species accumulation curve based on individuals) we made use of the "Sample Size-Based Rarefaction/Extrapolation" curves (with confidence intervals, Hsieh and Chao, 2019) calculated by means of the *iNext()* function from the "iNext" R package (Hsieh and Chao, 2019) and based on individuals numbers (in light of the small sample size of this survey, n=10). We produced two sets of graphs: i) Figure 6 a-d presents the rarefaction/extrapolation (R/E) curves (S_{est} and sample coverage) per taxon and taxonomic level (species and family) across the whole site B4S03.

3 Results

Average values are reported with their standard deviation. All results, including statistics, are reported in Table 1 a and b (main test and permdisp results) and in supplementary table ST3 a and b (permdisp and pair-wise tests).

3.1 Abiotic variables

The multivariate PERMANOVA based on the environmental variables (excl. pigments) did not find significant differences between stations but detected significant differences between layers (0-5 cm versus 5-10 cm layer), although the significant Permdisp test suggests caution in the interpretation of the significance of the main test (Table 1 a and ST3 a). When looking at single variables, the nodule coverage was significantly higher at the two nodule-rich stations compared to Nodfree. Nodule abundance (kg m^{-2}) statistical analysis showed a significant difference between the two nodule-rich and the nodule-free stations. The sediments of B4S03 site were dominated by silt (>70%) followed by clay (>15%) and sand (>6%) in all the investigated stations (Table 2). On the one hand, the percentage of sand and silt did not differ between stations and/or between layers. Clay%, on the other hand, displayed significant differences between Nodfree and Nodrich_A (higher clay content in Nodrich_A) and non-significant pair-wise t-test for Nodfree-Nodrich_B pair. Clay content showed the largest variance at Nodrich_B, which showed the highest clay content of the 0-5 cm layer, whereas Nodrich_A had higher clay content in the deeper layer. The median gran size (Median_GS) showed the largest variance at Nodrich_B with no significant differences between stations and/or layers. Porosity was higher in the upper 0-5 cm layer in all three stations. Total organic carbon (TOC%) ranged from a maximum of 0.62 ± 0.03% in Nodrich_A 0-5 cm layer to a minimum of 0.52 ± 0.03% in Nodfree 5-10 cm layer, displaying the largest variance in Nodrich_B, and showed a significant decrease with increasing sediment depth across all stations (Table 2). Total nitrogen (TN) and TOC/TN showed no significant differences between stations and/or the layer depth (Table 2).

The pigment concentrations in the sediment layers were all near detection level, with the highest values recorded at Nodfree for Chl-a and CPE and at Nodrich_B for phaeopigments. The univariate Chlorophyll-

293 a analysis tested significant for the interaction factor, but when the pair-wise t-test was performed no
294 significantly different pairs were detected. This may be explained by the significant PermDisp and /or by
295 the low number of replicates (Table 1 a and ST3 a). The phaeopigments analysis also showed a signifi-
296 cant interaction factor with the 0-1 cm layer differing significantly from all other layers only within sta-
297 tion Nodfree. Again, the significant PermDisp test result urges caution in the interpretation of the signifi-
298 cant main test results. Likewise, the CPE analysis showed the same pattern with a significant interaction
299 factor and significant differences of the 0-1 cm layer from the deeper layers at the nodule-free station.
300 Again, differences in the dispersion of the group variances may be the cause for these significant differ-
301 ences.

302 Overall, when looking at the Principal Component Analysis for the surface layer (0-5 cm) in Figure 2, we
303 can observe how the two nodule-rich sites displayed a relatively larger within-station variability, with
304 Nodrich_B showing the largest confidence interval (c.i.) ellipse. Moreover, the two nodule-rich stations's
305 ellipses considerably overlapped and their centroids were also very close to each other. Nodfree's cen-
306 troid separated from the two nodule-rich stations's centroid along PC2 axis (explaining 26.5%) but the
307 ellipse also overlapped with Nodrich_B. The PCA therefore points to non-significant differences between
308 the stations based on the multivariate sediment characteristics of the surface layer front.

309 The Net Primary Production (NPP, Figure 3) was estimated from monthly-averaged surface for B4S03 site
310 from the period January 2015 - June 2017 and it shows a maximum NPP peak in May 2016 (about 360
311 mg C m^{-2} d^{-1}) and the lowest in September of the same year.

312 3.2 Macrofauna analysis

313 The macrofauna assemblages from B4S03 showed total macrofaunal densities (excl. meiofauna) of 176 ±
314 36 individuals m^{-2} at the nodule-free station, 178 ± 30 individuals m^{-2} at Nodrich_A and 147 ± 57 indi-
315 viduals m^{-2} Nodrich_B (see supplementary material Table ST2). The univariate Permanova showed no
316 significant differences between stations (Table 1 b and ST3 b). Both the maximum total density of 212
317 individuals m^{-2} and the minimum of 64 individuals m^{-2} were estimated from box-cores collected at the
318 southern nodule - rich station Nodrich_B. A total of 10 identified higher taxa were found across all sam-
319 ples (Table ST1). The dominant taxa were Polychaeta (average relative abundance: 52 ± 9.8% Nodfree;

48 ± 15.6% Nodrich_B; 65 ± 17.3% Nodrich_A), Tanaidacea (average relative abundance: 19 ± 5.3% Nodfree; 16 ± 6.4% Nodrich_B; 13 ± 13.6% Nodrich_A) and Isopoda (average relative abundance: 21 ± 12% Nodfree; 11 ± 6.7% Nodrich_B; 7 ± 2.8% Nodrich_A), which together on average comprised the 91%, 75% and 85% of the total fauna at Nodfree, Nodrich_B and Nodrich_A respectively. Finally, the multivariate analysis at the higher-taxon level of the macrofauna densities showed no statistically significant differences in assemblage composition between the three stations (Table 1 b).

3.2.1 Dominant taxa diversity and distribution

Combining all samples, at B4S03 site, a total of 89 species belonging to 35 families were identified across all three taxa (see Figure 4). Of these species, 49 were represented in the samples as singletons (> 50%), 20 doubletons and another 21 were encountered more than twice (Table 5, also see supplementary material ST4 for list of species). In general, for each of the identified taxa, the diversity indices (taxon richness (T or S), Shannon-Wiener H', Pileou's evenness J', the expected taxon number ET(n)) were estimated for species and family taxonomical level (see Table 3). No statistically significant differences were found between stations for any of the estimated diversity indices in any of the analyses for any of the taxa (Table 1 b).

Looking at species and family distribution across all stations combining the three taxa (Figure 4 d), we observed that the total number of species identified at the three stations was very similar (Nodfree = 42 species; Nodrich_B = 43 species; Nodrich_A = 42 species) whereas Nodrich_B showed the highest number of families (29) followed by Nodrich_A with 27 families and Nodfree with 23 families. In total 11 species were shared among the three stations, 23 species were unique to Nodrich_A, 21 to Nodrich_B and 18 to Nodfree. When looking at family level, 16 families out of 37 were shared among the three stations when the combined diversity was considered. Nodfree and Nodrich_B stations (the southernmost sampling locations) both showed 5 unique families (all of them singletons) and Nodrich_A displayed 3 unique families.

3.2.1.1 Isopoda

Of the 31 isopod individuals identified to species level, a total of 17 morphospecies belonging to five families was observed (Figure 5). Of these, only two were shared among the three stations (see Figure

347 4a), and 14 were unique across the stations (see Table ST4): 6 species (belonging to 4 families ; 4 were
348 singletons) were found only at the nodule-free station, another 6 (belonging to 2 families ; 3 were sin-
349 gletons) at the Nodrich_A and only 2 species (belonging to 2 families ; both were singletons) at No-
350 drich_B. The asymptotic diversity estimation based on the Chao1 estimator computed a total of 25 spe-
351 cies to be recorded in the B4S03 site across an estimated total of 7 families (Table 4). Based on this
352 number we can state to have collected 68% of the total expected isopod diversity based on the num-
353 bers of samples and individuals identified. If we were to estimate the total species diversity as computed
354 by the non-parametric asymptotic estimator Chao1 (g=1 as calculated with the Chao1 excel calculator
355 (Chao *et al.*, 2009), see Table 4), we would have to collect an additional 41 samples for a total of 126
356 individuals, or sample a total surface area of 13 m^2. If, as suggested by Chao *et al.* (2009) we were to
357 select a fraction of the total estimated diversity to encompass most taxa with more realistic sampling
358 objectives, we would need to sample 95% of the total estimated diversity (g= 0.95, Table 4), and, in our
359 case study, for Isopoda we would need an additional 33 individuals or a total of 21 samples (5 m^2) from
360 the site. The relative abundances of the six Isopoda families (Figure 5, Supplementary Table ST5) for the
361 B4S03 site were Desmosomatidae (37%) followed by Nannoniscidae (25%), Dendrotionidae (22%),
362 Thambematidae (9%), Haploniscidae (3%) and Macrostylidae (3%) The most dominant species were *Den-*
363 *drotion* species A (belonging to the family Dendrotionidae, rel. abundance 21%), *Eugerdella* species A
364 (belonging to the family Desmosomatidae, rel. abundance 9%) and *Thambema* species A (belonging to
365 the family Thambematidae, rel. abundance 9%).

366 *3.2.1.2 Polychaeta*

367 A total of 46 species belonging to 20 families have been delimited amongst the 104 polychaete individ-
368 uals found in our samples. Of these, only 7 species were shared between all stations (Figure 4b). No-
369 drich_A presented the highest number of unique species (15, of which 13 were singletons), followed by
370 Nodrich_B (9, all singletons) and Nodfree (6, of which two were singletons). The Chao1 asymptotic spe-
371 cies diversity (S_{Chao1}) estimator computed a total expected species richness of 74.8 species to be record-
372 ed across a total of 26 families (Table 4). We therefore collected 61% of the expected species diversity
373 and 76% of the expected family diversity during our current sampling effort. In order to collect the total

expected species richness (g=1, Table 4) we would need an additional 745 individuals from 72 samples comprising a sampled area of 20 m^2 in total. In order to reach 95% of the Chao1-expected total species diversity we would need to collect 336 individuals or 42 samples covering 11 m^2 in total. Species were evenly represented across the whole site, with most species representing less than 2% of the total identified individuals. The most dominant species for the B4S03 site were *Aurospio dibranchiata* ID #1457 (Spionidae, rel. abundance 9%), *Bathyglicinde* cf. *B. profunda* (Goniadidae, rel. abundance 7%), *Aurospio dibranchiate* ID #249 (Spionidae, rel.abundance 6%), *Prionospio* sp. (ID #268, family Spionidae, rel. abundance 6%), *Paraonides* sp. ID #397 (family Spionidae, rel. abundance 6%) and *Paralacydonia paradoxa* (only species of the family Paralacydoniidae, rel. abundance 4%). The most dominant families (Figure 5, Supplementary Table ST5) for the B4S03 site were Spionidae (30%), Cirratulidae (15%) and Goniadidae (10%) with the rest of the families representing each ≤ 5% of the total identified organisms.

3.2.1.3 Tanaidacea

The Tanaidacea comprised 28 morphospecies belonging to 9 families across 62 identified individuals, of which only 2 species were shared among all the stations, and 21 species were unique: 6 (3 singletons) only occurring at Nodfree station, 2 (both singletons) at Nodrich_A and 13 (11 singletons, and possibly 4 new genera) only occurring at Nodrich_B (Figure 4c, Tables 4, ST4). The Chao1 asymptotic diversity estimation for the B4S03 site resulted in 53.6 species which means that our current sampling effort accounted for 52% of the expected Tanaidacea diversity S_{Chao1}. The Chao1 estimator computed a total of 10.5 estimated families for the site, indicating the 80-90% of diversity expected was recorded with our sampling effort. If we were to sample the entire estimated species diversity S_{Chao1} (g=1, Table 4) additional 575 individuals from 93 box-cores and a total area of 26 m^2 would need to be sampled. When we would plan to sample 95% of S_{Chao1} (g=0.95, Table 4), we would need to collect an additional 155 individuals, or a total of 35 samples and 9 m^2 of area. When considering the whole B4S03 site, the majority of Tanaidacea species represented less than 4% of the total identified individuals. The most dominant species were *Forcipatia* sp. ID #6 (belonging to the family Leptognathiidae, rel. abundance 14%), *Thumidochelia* sp. ID #157 (from the family Akanthophoreidae, rel. abundance 8%), *Stenotanais* sp. (ID #59, from the family Akanthophoreidae, relative abundance 6%) and *Caudalonga* sp. ID #74 (from the family Colletteidae, rel. abundance 6%). The most dominant families were Akantophoreidae (32%), Leptognathiidae (19%), and Colletteidae (10%); as many as 18% of all tanaidaceans (represented by *Insociabilitanais sp.* ID #160 and *Tanabnormia sp.* ID #25) could not be classified to any of currently defined families and according to current

systematic are grouped as Paratanoidea family *incertae sedis* (see http://www.marinespecies.org/aphia.php?p=taxdetails&id=246697). In order not to lose information, we included this superfamily as family in the analysis.

4 Discussion

4.1 Abiotic variables

4.1.1 Sediment characteristics

In general, the B4S03 site sediments seemed to be relatively similar between the three stations. Likewise to other deep-sea abyssal plains and other areas within the CCFZ (Khripounoff *et al.*, 2006; Smith *et al.*, 2008a; De Smet *et al.*, 2017), the stations' sea bottoms were formed by about 90% of very fine particles (below 63 µm), of which the largest fraction was silt (4-63 µm, on average 72%). The concentrations of total organic carbon found within this study were comparable to those of another GSR contract site (B4N01 more to the west, TOC% = 0.54 ± 0.02, de Smet et al., 2017), but higher than those recorded during the previous expedition GSRNOD15A by De Smet et al. (2017) in the same site (B4S03, TOC% = 0.41 ± 0.01) and in another GSR contract site (B6S02 more to the east, TOC% = 0.49 ± 0.02). Similarly, the values found within this study were larger than those recorded by Khripounoff et al. (2006, TOC% = 0.48) for the NIXO zone (Ifremer; 14° 02′ N, 130° 07′ W) within the CCFZ nodule fields. Across all analyses (multivariate and univariate) no consistent and/or significant differences between the two nodule-rich and the nodule-free sites were found, hence confirming our initial expectation. Nevertheless, from the PCA computed on the surface layer (0-5 cm, Figure 2) making use of all abiotic variables, we can observe how the nodule-rich stations' ellipses overlap significantly and their centroids segregate from that of the nodule-rich station ellipse. The ellipses incomplete segregation between the nodule-rich and nodule-free stations may be due to Nodrich_B large within-group variance and the overall low number of replication in a highly patchy environment (e.g. the sedimentary matrix) which in turn might hinder the detection of potentially meaningful differences in surface sedimentary features at the three sites.

4.1.2 Sedimentary total organic carbon as a proxy for POC flux

Sediment TOC in deep-sea sediments depends on the particulate organic carbon (POC) flux from the euphotic zone and the depth (Lutz *et al.*, 2007), with only part of the produced organic matter sinking on the seafloor (Smith *et al.*, 2018) and being mostly refractory in nature when reaching abyssal depths (Smith *et al.*, 2008b; Arndt *et al.*, 2013). The CCFZ is characterised by very low surface productivity which follows a gradient from higher to lower POC fluxes from east to west (Smith and Demopoulos, 2003). These POC fluxes are mirrored in the benthic abundances, which have also been reported to follow such westward decline along the CCFZ (Paul and Hecker, 1979; Smith *et al.*, 2008a; De Smet *et al.*, 2017; Wilson, 2017). Regional interannual and seasonal variability in surface primary production can be a possible explanation for the higher TOC values recorded at B4S03 during GSRNOD17 compared to GSRNOD15A (De Smet *et al.*, 2017). From the NPP satellite-derived primary productivity estimations (Figure 3) we can notice how the GSRNOD15A cruise (October 2015) took place about 20 weeks after a NPP peak of about 280 mg C m^{-2} d^{-1} in the area, whereas GSRNOD17 was conducted only eight weeks after a NPP peak of about 270 mg C m^{-2} d^{-1}. Smith *et al.* (2018) estimated that a time of 0-70 days is needed for surface primary production to be exported as POC to abyssal depths. Therefore, the residence time of the portion of NPP that would have reached our sediments in 2017 would have been shorter compared to the GSRNOD15A conditions. In the abyss of oligotrophic oceanic areas, the initial consumption of the organic matter fraction depositing on the surface sediment layer is expected to be done by bacteria, followed by surface protozoans (e.g., Gooday and Rathburn, 1999; Gooday, 2002; Sweetman *et al.*, 2019). In our study TOC decreased slightly yet significantly with increasing sediment depth across all three stations, pointing at both potential initial remineralisation and also to rather efficient vertical organic matter mixing, likely via bioturbation. Nevertheless, additional sampling is necessary to properly quantify the effective NPP that reaches the CCFZ nodule fields sediments (by using e.g. sediment traps) and their inhabiting biota since it represents valuable information for the understanding of the role that these ecosystems play in the global carbon flux and carbon sequestration in light also of the future of deep-sea mining in these areas (Straatmann et al. 2019).

4.2 Macrofauna assemblage structure and diversity

The soft sediment macrofauna investigated in this study showed no clear pattern in relation to the presence/absence of nodules. This contrasts with what Vanreusel *et al.* (2016) observed for epifaunal organisms in the CCFZ, where entire functional groups (mainly antipatharian corals and alcyonarians) were absent in nodule-free transects sampled by video surveys. In comparison with studies that used the same sampling gear (box-corer of 0.25 m^2 surface area) and investigated the same benthic component (soft sediment benthos), we can state that the average densities recorded for B4S03 macrofauna assem-

465 blage described here were relatively low compared to the abundances reported by Wilson et al. (2017)
466 for the western sites PRA (NOAA designated "Provisional Interim Protected Reserve Area", 774 ± 254 SD
467 ind. m^{-2}) and Domes C (370 ± 123 SD ind. m^{-2}) in the CCFZ, but in the same range of those reported in
468 the first baseline assessment for Dome C (152.44 ± 2.8 SE) by Hecker and Paul (1979). The sampling
469 effort was always much larger in these studies (Wilson et al., 2017: 71 box-corers at DOME C across
470 three sampling events; 16 box-corers at PRA; Hecker and Paul, 1979: 38 box-corers at DOME C) com-
471 pared to the present study. The observed relative abundances of the three dominant taxa are compara-
472 ble to those recorded elsewhere in the CCFZ, where Polychaeta were always the dominant group, fol-
473 lowed by either isopods or tanaids (Hessler and Jumars, 1974; Paul and Hecker, 1979; De Smet *et al.*,
474 2017; Wilson, 2017; Bonifácio *et al.*, 2020).

475 *4.2.1 Isopoda*

476 The same dominant families found in this study were highly representative for the GSR contract area's
477 B4S03, B4N01 and B6S02 sites investigated during a previous sampling cruise GSRNOD15A by De Smet
478 *et al.*, (2017). During that study, the authors identified some families of isopods not encountered
479 (Ischnomesidae) or encountered in significantly lower overall relative abundances (Macrostylidae) in the
480 present study. During GSRNOD15A, the Macrostylidae, represented mostly by *Macrostylis metallicola*
481 (Riehl and De Smet 2020), were found to be relatively abundant across the three sites of the GSR con-
482 tract area. In the present sampling the entire family was found to show much lower relative abundance
483 when considering B4S03 as a whole, and the most representative species was confirmed to be *Macro-*
484 *stylis metallicola* by 16S rRNA barcoding analysis (Riehl and De Smet 2020). The low relative presence of
485 Macrostylidae is surprising considering that in other CCFZ areas (Janssen *et al.*, 2015, 2019; De Smet *et*
486 *al.*, 2017) and in abyssal sediments in general (e.g., Wilson, 2008; Elsner *et al.*, 2015) this family is often
487 one of the most abundant isopod groups. Considering their occurrence in virtually all open-ocean abys-
488 sal sediments studied with appropriate gear (e.g., box-corer or epibenthic sledge;) as well as patchy dis-
489 tributions of abyssal macrofauna (Kaiser *et al.*, 2007; Jóźwiak *et al.*, 2020) the absence of Macrostylidae
490 from our samples (specifically from the nodule-rich stations) is probably due to under-sampling.

The family Ischnomesidae was absent during our sampling effort across all stations. De Smet *et al.*, (2017) observed Ischnomesidae in B6S02; however, it was absent in GSR sites B4S03 and B4N01 during the GSRNOD15A cruise sampling. Ischnomesidae species distribution and population structure has been investigated in the North West Pacific where an abyssal trench (with hadal depths of maximum 9604 m) is known to constitute a dispersal barrier for many of the isopod species found in the area (Bober *et al.*, 2019). The authors found that hadal species of Ischnomesidae had a poor dispersal ability at distances larger than about 300 km (Bober *et al.*, 2019) and that no lineages were found to cross the trench. The distance between B4S03 and B6S02 is about 300 km, potentially indicating that if species belonging to this family have very little dispersal potential, their distribution may be limited to specific parts of the GSR contract area. Nevertheless, more information on POC fluxes and bottom currents' strength and direction are needed to understand species distribution. Further, like in Macrostylidae, expansion of ischnomesid populations into our study area could have easily occurred over long time spans outweighing the low-dispersal argument, and the lack of large deep-sea mountain chains between the two GSR contract sites (B6S02 and B4S03) would support this opposition. Other isopod families that could have been expected in the samples but was represented neither in our nor in De Smet *et al.*'s (2017) samples are the Munnopsidae and Haploniscidae. Munnopsidae was, however, found in the CCFZ by Janssen *et al.* (2015) in a study based on epibenthic sled samples. Most munnopsids are highly motile and have a rather epibenthic or hyperbenthic lifestyle and Haploniscidae have an epibenthic lifestyle as well. In abyssal epibenthic sledge samples these groups are often dominating the isopod fraction of the macrofauna (Meyer-Löbbecke *et al.*, 2014; Golovan *et al.*, 2019) but not so in box-corer samples (Wilson, 2008) indicating a gear-dependent bias. Previous studies showed that epibenthic isopods are more affected by turbulence than inbenthic groups (Thistle and Wilson, 1987, 1996). The box-corer creates a bow-wave effect before touch down which may affect the epibenthic groups thus reducing their representation while the epibenthic sledge may underrepresent inbenthic groups sliding on the sediment surface (Jóźwiak *et al.*, 2020). We hence consider sampling bias to be the most likely explanation for Ischnomesidae to be absent from our samples. A lack of representation of two isopod families is supported by our estimation of isopod diversity in the area.

De Smet *et al.* (2017) collected 12 box-corer samples during GSRNOD15A in two GSR contract sub-areas (B4 and B6) at three stations within the sites B4S03, B4N01, B6S02. The authors recorded 18 isopod species with only 11% of the taxa being shared across the three sites, and computed a S_{Chao1} of 26 species. Considering the high patchiness of abyssal Asellota (Kaiser *et al.*, 2007; Wilson, 2008) and the large distance (250-300 km) between the three sites, we can presume that the Chao1 diversity estimator underestimated the species diversity during the study of De Smet *et al.* (2017), because during the current study which is based on 10 box-corer samples, we recorded in B4S03 a total of seventeen species and estimated a species richness of 25 species. However, as discussed above, number of box-corers used during our investigation are yet to be considered limited in light of the low abundances and distribution of deep-sea isopods. This renders our results prone to sampling bias and may still limit our capacity to accurately estimate isopod diversity and distributional patterns, with an overall overestimation of endemism and an underestimation of the total local and regional diversity.

4.2.2 Polychaeta

The dominance of spionids among other Polychaeta families had been already observed by (Bonifácio *et al.*, 2020) during a much more intensive (30 box-corer samples) and extensive sampling (five areas over 1440 km along the eastern side of the CCFZ). In particular, during their study, spionids were dominant across the eastern Ifremer (34%), GSR (B6S02 site, 27%) and IOM (19%) contract areas, whereas the protected area APEI#3 (Area of Particular Ecological Interest) and the contract area BGR were dominated by the cirratulids, the second most dominant group in our investigation. Interestingly, these authors observed a turnover in the species composition between the eastern sites (BGR, IOM and GSR), characterized by a lumbrinerid species, and the western locations (eastern Ifremer and APEI#3), characterised by spionids, cirratulid, paraonid, maldanid and opheliid. Also Smith et al. (2008) described the biodiversity and species range of polychaetes in the CCFZ comparing an eastern (E site, centered at ~15° N, 119° W, in specific the IOM contract area), a central (C site, centred at ~ 14°5′ N, 130° 5′ W or the eastern Ifremer contract area) and a western (W site, located at 9° 33′ N, 150° 0.5′ W, the western Ifremer contract area) sites. In this study the authors found that in the eastern site Lumbrineridae and Amphinomidae were the most dominant families. The central and western sites (E and W) instead showed an

546 assemblage dominated by Spionidae, Cirratulidae, Syllidae and Paraonidae, with Spionidae displaying
547 relative abundances comparable to the values observed in the present study. In our studies Amphino-
548 midae were not recorded and Lumbrineridae were found in very low relative abundances (3%). As sug-
549 gested by Smith *et al.* (2008b) and supported by Bonifácio *et al.* (2020), the dominance of jawed carni-
550 vores such as lumbrinerids, amphinomids and sigalionids in the eastern side reinforces the expected
551 higher surface productivity of this region of the CCFZ, for the development of higher trophic levels
552 needs a relatively high abundance of prey. The GSR contract area is composed of an i) eastern sub-area,
553 B6, of which the B6S02 site was sampled by De Smet *et al.* (2017) during the GSRNOD15A sampling
554 campaign, ii) a central sub-area, B4 of which B4S03 was sampled during both GSRNOD15A and the cur-
555 rent study GSRNOD17 cruise, and iii) an western sub-area B2, which was sampled in a non-quantitative
556 and replicated fashion during GSRNOD14, and for which no macrofauna data is available. In De Smet *et*
557 *al.* (2017) the Polychaeta family composition displayed a significantly higher presence of Lumbrineridae
558 at the eastern-most site B6S02 compared to the other two B4 investigated stations where the family was
559 only represented in two out of nine box-cores and in very low relative abundances. In the B6S02 site the
560 family was found in each sample and it comprised 20% of the assemblage. From this evidence we can
561 assume that the polychaete diversity patterns in the sub-areas of the GSR contract area follow the previ-
562 ously described east-west gradient in productivity (Smith *et al.*, 2008a; Volz *et al.*, 2018); the site under
563 current investigation (B4S03) is part of the central zone of the CCFZ where higher trophic levels can be
564 expected to occur infrequently because of the low overall food availability and this is reflected in the
565 dominance of polychaete deposit feeder families (e.g. Spionids) and the virtual absence of predator
566 families observed in the current study.

567 During GSRNOD15A De Smet et al., (2017) recorded a total of 53 polychaete taxa (at genus and species
568 level) for B4 (B4S03 and B4N01 sites) and B6 (B6S02 station) GSR contract sub-areas, of which only 26%
569 of the taxa were shared between the three stations. When the authors computed the asymptotic diversi-
570 ty S_{Chao1} the result pointed at a total of 77 taxa to be found across the different sites with an increasing
571 number of samples, based on an overall sampling effort of 12 box cores. During the current study, we
572 found 46 species from a total of ten box cores at the B4S03 site. It would therefore seem that the Chao1
573 non-parametric diversity estimator underestimated the potential diversity of the GSR sites during the

work of De Smet *et al.* (2017), because during the present study we found a total of 46 species and an estimated S_{Chao1} of 74.8 species for the sole B4S03 site. In our study, and in that of other authors (Bonifácio *et al.*, 2020), the number of polychaete singletons did not decrease with the increasing number of box-corers sampled, as 52% of the polychaete species found across all box-cores were singletons. Further, during this study polychaete morphospecies distribution within B4S03 and across the investigated stations (Figure 4 b) showed a higher degree of uniqueness (15 unique species out of 46) at Nodrich_A which is the northern-most and most distant station relative to the other two southern stations. Nonetheless, Nodfree and Nodrich_B are both located at the south of B4S03 and only 3 km apart from each other and they showed the highest number of shared morphospecies (7 out of 46). This observation may point at a higher dispersal potential across shorter distances for polychaete larvae at these depths. Previous studies showed that in comparison to isopods, polychaetes indeed have a slightly better potential for dispersal (Janssen *et al.*, 2015, 2019). Bonifácio et al. (2020) estimated a polychaete diversity that could range from 498 species (estimated by Chao1 estimator) to 240,000 species (based on species turnover rates) for the 6 million km^2 of the CCFZ region. Ongoing and future baseline studies in the CCFZ nodule fields need to focus on gathering more species distributional data for dominant taxa such as Polychaeta to be able to estimate and hence mitigate the effects that potential habitat fragmentation resulting from the nodule harvesting activities could have on the distribution and dispersal of species.

4.2.3 Tanaidacea

There are few studies dedicated to tanaidacean diversity and describing their community in the CCFZ. In the analysis of macrofauna assemblages in DOMES site A and site C (ECHO1), only six tanaidacean families were recorded: Leptognathiidae, Pseudotanaidae, Agathotanaidae, Anarthruridae, Neotanaidae and Whitellegidae (Wilson, 1987). The 77 species of Tanaidacea recorded by Wilson (1987; 2017) (Wilson, 1987, 2017)could be classified to at least nine families (Agathotanaidae, Akanthophoreidae, Apseudidae, Colletteidae, Leptognathiidae, Neotanaidae, Pseudotanaidae, Paranarthrurellidae and Typhlotanaidae). Błażewicz et al. (2019) in a study that covered the contract areas of BGR, IOM, GSR, Ifremer and the Area of Particular Environmental Interest APEI#3, recorded a high tanadacean diversity comparable to the present study. The unique character of each area was proved based on molecular data for the only

tanaidacean family (Pseudotanaidae) that was present at each of the mentioned areas (Jakiel *et al.*, 2019). Further, Błażewicz *et al.* (2019) reported a total of 22 species from 5 box-corers samples taken at GSR B6S02 site at depths around 4500 m. The authors stated that most species were unique to one area and that 47% were singletons. A species list was not provided in the work hence comparisons with the current study on B4S03 cannot be made at the moment. A high degree of licence area-specific morphospecies distribution was also detected by Błażewicz et al. (2019) when comparing far distant contract areas within the CCFZ nodule fields. In our study we identified one morphospecies which was assigned to the genus *Neotanais* (Neotanaidae family, *Neotanais sp.* #161), recorded only once (singleton) and which was unique to Nodfree station. The genus *Neotanais* has been sampled by other authors during the JPIO cruise in the CCFZ and it displayed very high genetic diversity with 4 individuals all representing four new species (Magda Błażewicz, personal communication). Moreover, during this study the specialist taxonomist found four new genera and a potentially new family.

Tanaidacea are among the least known deep-sea taxa. Their densities in the deep sea are thought to be under-estimated and their importance in the macrobenthic community seems to be comparable to that of isopods or amphipods (Błażewicz-Paszkowycz *et al.*, 2012; Jakiel *et al.*, 2019). For the greater part free-living tanaids are known to live into self-constructed tubes or buried in sediments and to display a brooding reproduction type (Jakiel *et al.*, 2019 and references therein). Characterised by the lack of larval phase and in light of their low mobility, they are known to have a low dispersal capacity, although active stages and opportunist benthopelagic forms such as the "swimming male" of *Leptoghnathia* sp., Kudinova-Pasternak 1970, have been mentioned as likely early colonisers of deep-sea disturbed sediments at great depths (Bird and Holdich, 1989; Błażewicz-Paszkowycz *et al.*, 2014) or important element sustaining the population connectivity in the scarcely distributed and infrequent deep-sea population. The high diversity measured for this taxon at B4S03 and a substantial contribution of individuals identified only to superfamily level (Paratanaoidea/family *incertae sedis*), stay in line with a high diversity of the tanaidacean recorded in the deep-sea (Błażewicz-Paszkowycz *et al.*, 2012; Poore *et al.*, 2015) and it is in line with the typical high diversity recorded in the deep sea for other taxa (Rex and Etter 2010) and general underestimation of the small marine peracarids (Appeltans *et al.*, 2012). Nonetheless the high number of singletons can again be a sign of under-sampling, a risk for diversity under-estimation and the low den-

629 sities and high patchiness in the distribution of these organisms can instead over-estimate the level of
630 specificity and endemism of the identified morphospecies.

631 4.3 Baseline ecological assessment in highly diverse ecosystems: diversity estimation 632 limitations and implications for sampling design

633 The analysis of diversity estimation for the three main taxa highlighted a common trend: a high number
634 of singletons not declining with an increasing number of samples. The use of the Chao1 estimator,
635 which takes in consideration the number of singletons and doubletons, may not be fit for highly diverse
636 ecosystems such as the deep sea, for this asymptotic estimator assumes that the number of singletons
637 will decrease with increasing number of samples (Melo, 2004). In this study, for isopods as for the other
638 two taxa, the number of singletons was >50%, with one in two individuals representing a new species
639 which would be encountered only once across all samples. Very high levels of singletons are a character-
640 istic of most deep-sea ecosystems (excl. chemosynthetic ecosystems), where rare and common species
641 contribute to an equal 25% of all singletons (Rex and Etter, 2010) and one on three macrofauna organ-
642 isms in a sampling area is a singleton (Gage, 2004). Coddington *et al.* (2009) recorded, for the spider
643 population of a large area of rain forest, a very high number of singletons (26%) during an intensive
644 survey. The authors concluded that this result was most likely due to under-sampling in a highly diverse
645 ecosystem, generating negative biases for diversity estimators. Under-sampling can hence cause an un-
646 derestimation of diversity, but at the same time it can overestimate the level of endemism and hence
647 produce an illusionary narrowness of the effective distribution range of species, as 1/3 of the species are
648 potentially singletons and would then be considered endemic to a specific area.

649 The environmental impact assessment (EIA) outlined by the International Seabed Authority is a prerequi-
650 site to Deep-Sea Mining activities in areas beyond national jurisdiction such as the CCFZ. The require-
651 ments for the EIA are, righteously, particularly detailed and demanding in terms of in-depth information
652 on the baseline status of the local ecosystem and of the potential effects nodule harvesting activities
653 may have on these remote biomes of the Earth's ocean floor. The deep-sea nodule fields of the CCFZ
654 represent a yet very understudied ecosystem that spans for about 6 million square kilometres at abyssal
655 depths in the North Central Pacific Ocean and which are logistically impervious to investigate thorough-

656 ly. From the yet limited information gathered in the present study and with the knowledge gathered
657 from other studies in the area, it is clear that the local diversity is most likely highly underestimated by
658 each of the sampling campaigns that have been carried out to date in the region. In Figure 6 we find
659 the rarefaction/extrapolation (R/E) curves (with 95% confidence intervals) for the different taxa (a,b) and
660 the related sample coverage (SC; c,d) for species and family level. For most taxa the SC is relatively high
661 at the family level, with Tanaidacea showing a value approaching SC = 1, followed by the Isopoda and
662 the Polychaeta. At the species level the extrapolated S_{est} shows how the Polychaeta require a larger
663 sampling compared to the Tanaidacea and Isopoda and that no asymptote will be reached when a total
664 of 200 polychaete individuals will have been sampled at B4S03 (Figure 6 c). The estimation for necessary
665 additional sampling effort in order to cover the complete (estimated) biodiversity reached as many as
666 126 individuals for Isopoda, 745 individuals for Polychaeta and 575 individuals for Tanaidacea. Further, to
667 record 100% (g=1) of the estimated diversity (which can be assumed being under-estimated for each of
668 the three taxa in light of the high percentage of singletons), we would need five times the sampling
669 effort for Isopoda, eight times for Polychaeta and ten times for Tanaidacea (Table 4). To make sure the
670 most vulnerable taxa are sufficiently represented, which are the ones with the lowest dispersal capacity
671 such as the Asellota Isopoda or the highly diverse Tanaidacea, a five- to ten-fold sampling effort in the
672 B4S03 site is required. In the case we would achieve the minimum required sampling to estimate the
673 total diversity of the Asellota as per this investigation, we would need to sample five times the original
674 sampling area or collect a total of 50 box-cores. In this case we would be able to record the Isopoda
675 S_{Chao1} (g = 1) diversity, whereas for Polychaeta and Tanaidacea we would reach an estimated g ≥ 0.95.

676 Therefore, a more comprehensive sampling strategy is needed to estimate the full diversity of sites such
677 as B4S03, though a moderate increase in sampling may be sufficient to characterize higher taxon level
678 community structure.

679 To fully characterize local diversity to the lowest taxonomic level, future sampling campaigns would ide-
680 ally need to carry out an improved comprehensive type of sampling design and focus on B4S03 and/or
681 B6S02 (GSR sites with most information available) to unravel the local diversity coupling molecular tools
682 and lower taxonomic level identification by taxonomic experts. Further, the study should relate the diver-

sity to each sites' habitat/environmental characteristics in order to identify potentially important drivers and to finally be able to unravel connectivity patterns of selected taxa with different dispersal potential between the two sites.

5 Conclusions

The macrofauna of the B4S03 site within the GSR contract area is highly diverse. The presence of nodules did not affect either the soft sediment characteristics or the biological assemblage in an obvious way. The densities of the local macrofauna or the diversity of Isopoda, Polychaeta and Tanaidacea did not significantly differ between the investigated stations, nor did the overall macrofauna assemblage structure with polychaetes dominating the abundances followed by tanaids and isopods. The high number of singletons encountered during the study may be a sign of under-sampling and a risk for diversity underestimation at the investigated sites. In light of the requirements for the Environmental Impact Assessment outlined by the International Seabed Authority, contractors need to be able to properly estimate the local diversity to then mitigate the effects that potential habitat fragmentation resulting from the harvesting activities could have on the local survival of species. The understanding of diversity patterns at the different spatial scales (from local to regional) is paramount to the proper management of deep-sea mining in the CCFZ region. We recommend a more extensive sampling design but also complementary analytical effort with the combination of molecular tools with taxonomical expertise to fully characterize biodiversity (including cryptic species) and to identify connectivity patterns crucial for management of deep-sea mining activities.

6 Authors contribution

Francesca Pasotti analysed and interpreted the data, produced and organised the results and wrote the manuscript. Lisa Mevenkamp helped with the analysis and data interpretation, carried out most of the after-cruise sample processing and did part of the lower-taxon identification with the help of the expert taxonomists. Ellen Pape coordinated the sampling design, helped with the data analysis, the interpretation of the results and the review of the manuscript. Lidia Lins and Bart De Smet carried out the

GSRNOD17 sampling and helped in reviewing the present manuscript. Nene Lefaible helped in reviewing the manuscript and processed part of the macrofauna samples. Blażewicz-Paszkowycz identified the Tanaidacea up to lower taxon level, Torben Riehl the Isopoda, and Paulo Bonifácio identified the Polychaeta. All the expert taxonomists helped in the interpretation of the data and the review of the manuscript. Ann Vanreusel is the project leader and helped in the sampling design, the data analyses and interpretation and the writing of the manuscript.

7 Acknowledgments

The authors wish to extend their gratitude and appreciation to the captain and (scientific) crew of the RV "Topaz Captain" as well as OFG for the help on board during the GSRNOD17 cruise. We also wish to acknowledge the exploration manager and chief scientist François Charlet (GSR). The help of Céline Taymans (GSR) and Tania Nara Bezerra (UGent) with onboard sample processing was greatly appreciated. Further, we wish to thank Hannah Wright who helped with the identification of macrofauna to higher-taxon level. Bruno Vlaeminck and Bart Beuselinck are acknowledged for their help with the environmental variable analysis. This investigation was part of the environmental baseline survey carried out by GSR within its contract area and it was supported by a service arrangement between Global Sea Mineral Resources N.V. and Ghent University.

8 References

Amon, D. J., Ziegler, A. F., Dahlgren, T. G., Glover, A. G., Goineau, A., Gooday, A. J., Wiklund, H., *et al.* 2016. Insights into the abundance and diversity of abyssal megafauna in a polymetallic-nodule region in the eastern Clarion-Clipperton Zone. Scientific Reports, 6: 30492.

Amon, D. J., Ziegler, A. F., Drazen, J. C., Grischenko, A. V., Leitner, A. B., Lindsay, D. J., Voight, J. R., *et al.* 2017. Megafauna of the UKSRL exploration contract area and eastern Clarion-Clipperton Zone in the Pacific Ocean: Annelida, Arthropoda, Bryozoa, Chordata, Ctenophora, Mollusca. Biodiversity Data Journal. https://www.ncbi.nlm.nih.gov/pmc/articles/PMC5565845/ (Accessed 26 September 2018).

Appeltans, W., Ahyong, S. T., Anderson, G., Angel, M. V., Artois, T., Bailly, N., Bamber, R., *et al.* 2012. The Magnitude of Global Marine Species Diversity. Current Biology, 22: 2189–2202.

Arndt, S., Jørgensen, B. B., LaRowe, D. E., Middelburg, J. J., Pancost, R. D., and Regnier, P. 2013. Quantifying the degradation of organic matter in marine sediments: a review and synthesis. Earth-Science Reviews, 123: 53–86.

Balaram, V. 2019. Rare earth elements: A review of applications, occurrence, exploration, analysis, recycling, and environmental impact. Geoscience Frontiers, 10: 1285–1303.

Behrenfeld, M. J., and Falkowski, P. G. 1997. Photosynthetic rates derived from satellite-based chlorophyll concentration. Limnology and Oceanography, 42: 1–20.

Bird, G. J., and Holdich, D. M. 1989. Recolonisation of artificial sediments in the deep bay of Biscay by Tanaidaceans (Crustacea: Peracarida), with a description of a new species of Pseudotanais. Journal of Marine Biological Association U.K., 69: 307–317.

Błażewicz, M., Jóźwiak, P., Menot, L., and Pabis, K. 2019. High species richness and unique composition of the tanaidacean communities associated with five areas in the Pacific polymetallic nodule fields. Progress in Oceanography, 176: 102141.

Błażewicz-Paszkowycz, M., Bamber, R., and Anderson, G. 2012. Diversity of Tanaidacea (Crustacea, Peracarida) in the World's ocean: how far have we come? Plos One, 7.

Błażewicz-Paszkowycz, M., Jennings, R. M., Jeskulke, K., and Brix, S. 2014. Discovery of swimming males of Paratanoidea (Tanaidacea). Polish Polar Research, 35: 415–453.

Bober, J., Brandt, A., Frutos, I., and Schwentner, M. 2019. Diversity and distribution of Ischnomesidae (Crustacea: Isopoda: Asellota) along the Kuril-Kamchatka Trench – A genetic perspective. Progress in Oceanography, 178: 102174.

Bonifácio, P., and Menot, L. 2019. New genera and species from the Equatorial Pacific provide phylogenetic insights into deep-sea Polynoidae (Annelida). Zoological Journal of the Linnean Society, 185: 555–635.

Bonifácio, P., Martínez Arbizu, P., and Menot, L. 2020. Alpha and beta diversity patterns of polychaete assemblages across the nodule province of the eastern Clarion-Clipperton Fracture Zone (equatorial Pacific). Biogeosciences, 17: 865–886. Copernicus GmbH.

Burns, R. G., and Burns, V. M. 1977. The mineralogy and crystal chemistry of deep-sea manganese nodules, a polymetallic resource of the twenty-first century. Philosophical Transactions of the Royal Society of London, 286: 283–301.

Bussau, C. 1993. Taxonomische und ökologische untersuchungen an Nematoden des Peru-Beckens. na.

Chao, A., Colwell, R. K., Lin, C.-W., and Gotelli, N. J. 2009. Sufficient sampling for asymptotic minimum species richness estimators. Ecology, 90: 1125–1133.

Chao, A., Gotelli, N. J., Hsieh, T. C., Sander, E. L., Ma, K. H., Colwell, R. K., and Ellison, A. M. 2014. Rarefaction and extrapolation with Hill numbers: a framework for sampling and estimation in species diversity studies. Ecological Monographs, 84: 45–67.

Christodoulou, M., O'Hara, T. D., Hugall, A. F., and Arbizu, P. M. 2019. Dark ophiuroid biodiversity in a prospective abyssal mine field. Current Biology, 29: 3909–3912.

Coddington, J. A., Agnarsson, I., Miller, J. A., Kuntner, M., and Hormiga, G. 2009. Undersampling bias: the null hypothesis for singleton species in tropical arthropod surveys. Journal of Animal Ecology, 78: 573–584.

De Smet, B., Pape, E., Riehl, T., Bonifácio, P., Colson, L., and Vanreusel, A. 2017. The Community Structure of Deep-Sea Macrofauna Associated with Polymetallic Nodules in the Eastern Part of the Clarion-Clipperton Fracture Zone. Frontiers in Marine Science, 4. http://journal.frontiersin.org/article/10.3389/fmars.2017.00103/abstract (Accessed 11 April 2017).

Dover, C. L. V., Ardron, J. A., Escobar, E., Gianni, M., Gjerde, K. M., Jaeckel, A., Jones, D. O. B., *et al.* 2017. Biodiversity loss from deep-sea mining. Nature Geoscience, 10: 464–465.

Elsner, N. O., Malyutina, M. V., Golovan, O. A., Brenke, N., Riehl, T., and Brandt, A. 2015. Deep down: isopod biodiversity of the Kuril-Kamchatka abyssal area including a comparison with data of previous expeditions of the RV Vityaz. Deep-Sea Research II, 111: 210–219.

Gage, J. D. 2004. Diversity in deep-sea benthic macrofauna: The importance of local ecology, the larger scale, history and the Antarctic. Deep-Sea Research Part II: Topical Studies in Oceanography, 51: 1689–1708.

Gehlenborg, N. 2019. UpSetR: A More Scalable Alternative to Venn and Euler Diagrams for Visualizing Intersecting Sets. https://CRAN.R-project.org/package=UpSetR.

Gheerardyn, H., and George, K. H. 2019. Description of a new species of Neoargestes Drzycimski, 1967 (Copepoda, Harpacticoida, Argestidae) from the Clarion Clipperton Fracture Zone (Pacific Ocean), with remarks on the systematics of the genus. Marine Biodiversity. https://doi.org/10.1007/s12526-019-00951-1 (Accessed 6 May 2019).

Giere, O. 2009. Meiobenthology: the microscopic motile fauna of aquatic sediments. Springer-Verlag, Berlin. 527 pp. file:///D:/Elpape/My Documents/Ellen.Data/PDF/Giere_Meiobenthology_2009-2871546624/Giere_Meiobenthology_2009.pdf.

Glover, A. G., and Smith, C. R. 2003. The deep-sea floor ecosystem: current status and prospects of anthropogenic change by the year 2025. Environmental Conservation, null: 219–241.

Golovan, O. A., Błażewicz, M., Brandt, A., Jażdżewska, A. M., Jóźwiak, P., Lavrenteva, A. V., Malyutina, M. V., *et al.* 2019. Diversity and distribution of peracarid crustaceans (Malacostraca) from the abyss adjacent to the Kuril-Kamchatka Trench. Marine Biodiversity, 49: 1343–1360.

Gooday, A., and Rathburn, A. 1999. Temporal variability in living deep-sea foraminifera: a review. Earth Science Reviews, 46: 187–212.

Gooday, A. 2002. Biological responses to seasonally varying fluxes of organic matter to the ocean floor: a review. Journal of Oceanography, 58: 305–332.

Goslee, S., and Urban, D. 2020. ecodist: Dissimilarity-Based Functions for Ecological Analysis. https://CRAN.R-project.org/package=ecodist.

Hervé, M. 2020. RVAideMemoire: Testing and Plotting Procedures for Biostatistics. https://CRAN.R-project.org/package=RVAideMemoire.

Hessler, R. R., and Jumars, P. A. 1974. Abyssal community analysis from replicate box cores in the central North Pacific. Deep Sea Research and Oceanographic Abstracts, 21: 185–209.

Hsieh, T. C., Ma, K. H., and Chao, A. 2016. iNEXT: an R package for rarefaction and extrapolation of species diversity (Hill numbers). Methods in Ecology and Evolution, 7: 1451–1456.

Hsieh, T. C., and Chao, A. 2019. Package iNEXT 2.0.19: interpolation and extrapolation of species diversity. http://chao.stat.nthu.edu.tw/blog/software-download/.

Hurlbert, S. H. 1971. The nonconcept of species diversity: a critique and alternative parameters. Ecology, 52: 577–586.

Jakiel, A., Palero, F., and Błażewicz, M. 2019. Deep ocean seascape and Pseudotanaidae (Crustacea: Tanaidacea) diversity at the Clarion-Clipperton Fracture Zone. Scientific Reports, 9: 1–49.

Janssen, A., Kaiser, S., Meißner, K., Brenke, N., Menot, L., and Martínez Arbizu, P. 2015. A Reverse Taxonomic Approach to Assess Macrofaunal Distribution Patterns in Abyssal Pacific Polymetallic Nodule Fields. PLoS ONE, 10: e0117790.

Janssen, A., Stuckas, H., Vink, A., and Arbizu, P. M. 2019. Biogeography and population structure of predominant macrofaunal taxa (Annelida and Isopoda) in abyssal polymetallic nodule fields: implications for conservation and management. Marine Biodiversity. https://doi.org/10.1007/s12526-019-00997-1 (Accessed 2 October 2019).

Jóźwiak, P., Pabis, K., Brandt, A., and Błażewicz, M. 2020. Epibenthic sled versus giant box corer – Comparison of sampling gears for tanaidacean species richness assessment in the abyssal benthic ecosystem. Progress in Oceanography, 181: 102255.

Juan, C., Van Rooij, D., and De Bruycker, W. 2018. An assessment of bottom current controlled sedimentation in Pacific Ocean abyssal environments. Marine Geology, 403: 20–33.

Kaiser, S., Barnes, D. K. A., and Brandt, A. 2007. Slope and deep-sea abundance across scales: Southern Ocean isopods show how complex the deep sea can be. Deep-Sea Research II, 54: 1776–1789.

Kersken, D., Janussen, D., and Arbizu, P. M. 2019. Deep-sea glass sponges (Hexactinellida) from polymetallic nodule fields in the Clarion-Clipperton Fracture Zone (CCFZ), northeastern Pacific: Part II—Hexasterophora. Marine Biodiversity, 49: 947–987.

Khripounoff, A., Caprais, J. C., Crassous, P., and Etoubleau, J. 2006. Geochemical and biological recovery of the disturbed seafloor in polymetallic nodule fields of the Clipperton-Clarion Fracture Zone (CCFZ) at 5,000-m depth. Limnology and Oceanography, 51: 2033–2041.

Lutz, M. J., Caldeira, K., Dunbar, R. B., and Behrenfeld, M. J. 2007. Seasonal rhytms of net primary production and particulate organic carbon flux describe biological pump efficiency in the global ocean. Journal of Geophysical Research, 112.

Maybury, C. 1996. Crevice Foraminifera from abyssal South East Pacific manganese nodules. *In* Microfossils and Oceanic Environments. Ed. by Moguilevsky.

Melo, A. S. 2004. A critique of the use of jackknife and related non-parametric techniques to estimate species richness. Community Ecology, 5: 149–157.

Meyer-Löbbecke, A., Brandt, A., and Brix, S. 2014. Diversity and abundance of deep-sea Isopoda along the Southern Polar Front: Results from the SYSTCO I and II expeditions. Deep Sea Research Part II: Topical Studies in Oceanography, 108: 76–84.

Michael J. Rex, and Ron J. Etter. 2010. Deep-sea Biodiversity: Pattern and Scale. Harvard University Press, Cambridge, Massachussets. 354 pp.

Miljutin, D., Miljutina, M., and Messié, M. 2015. Changes in abundance and community structure of nematodes from the abyssal polymetallic nodule field, Tropical Northeast Pacific. Deep Sea Research Part I: Oceanographic Research Papers, 106: 126–135.

Murray, J., and Renard, Rev. A. F. 1891. Report on deep-sea deposits based on the specimens collected during the voyage of the H.M.S. Challenger in the years 1872 to 1876. Order of her Majesty Office.

Oksanen, J., Blanchet, F. G., Friendly, M., Kindt, R., Legendre, P., McGlinn, D., Minchin, P. R., *et al.* 2019. vegan: Community Ecology Package. https://CRAN.R-project.org/package=vegan.

Pape, E., Bezerra, T. N., Gheerardyn, H., Buydens, M., Kieswetter, A., and Vanreusel, A. In prep. Are polymetallic nodules important for deep-sea meiofauna?

Pape, E., De Smet, B., Bogaert, K., and Vanreusel, A. 2016. Biological and environmental report on the 2014 and 2015 expeditions in the GSR license area. Marine Biology Research Group, Ghent University, Ghent, Belgium.

Paul, A. Z., and Hecker, B. 1979. Abyssal Community Structure of the Benthic Infauna of the Eastern Equatorial Pacific: DOMES Sites A, B, and C. *In* Marine Geology and Oceanography of the Pacific Manganese Nodule Province, pp. 287–308. Ed. by J. L. Bischoff and D. Z. Piper. Springer US. http://link.springer.com/chapter/10.1007/978-1-4684-3518-4_8 (Accessed 8 October 2014).

Pennington, J. T., Mahoney, K. L., Kuwahara, V. S., Kolber, D. D., Calienes, R., and Chavez, F. P. 2006. Primary production in the eastern tropical Pacific: A review. Progress in Oceanography, 69: 285–317.

Petersen, S., Krätschell, A., Augustin, N., Jamieson, J., Hein, J. R., and Hannington, M. D. 2016. News from the seabed – Geological characteristics and resource potential of deep-sea mineral resources. Marine Policy, 70: 175–187.

Poore, G. C. B., Avery, L., Błażewicz-Paszkowycz, M., Browne, J., Bruce, N. L., Gerken, S., Glasby, C., *et al.* 2015. Invertebrate diversity of the unexplored marine western margin of Australia: taxonomy and implications for global biodiversity. Marine Biodiversity, 45: 271–286.

R Core Team. 2020. R: A Language and Environment for Statistical Computing. R Foundation for Statistical Computing, Vienna, Austria. https://www.R-project.org/.

Rex, M. A., and Etter, R. J. 2010. Deep-Sea Biodiversity: Pattern and Scale. Harvard University Press. 388 pp.

Riehl, T., Wilson, G. D. F., and Malyutina, M. V. 2014. Urstylidae – a new family of abyssal isopods (Crustacea: Asellota) and its phylogenetic implications. Zoological Journal of the Linnean Society, 170: 245–296.

Riehl, T., and De Smet, B. (n.d.). Macrostylis metallicola spec. nov. — An isopod with geographically clustered genetic variability from a polymetallic-nodule area in the Clarion-Clipperton Fracture Zone. in press.

Sanders, H. 1968. Marine benthic diversity: a comparative study. The American Naturalist, 102: 243.

Smith, C., and Demopoulos, W. R. 2003. The deep Pacific Ocean floor. *In* Ecosystems of the Deep Oceans, pp. 179–218. Elsevier Science, Amsterdam.

Smith, C. R., Hoover, D. J., Doan, S. E., Pope, R. H., Demaster, D. J., Dobbs, F. C., and Altabet, M. A. 1996. Phytodetritus at the abyssal seafloor across 10° of latitude in the central equatorial Pacific. Deep Sea Research Part II: Topical Studies in Oceanography, 43: 1309–1338.

Smith, C. R., Berelson, W., Demaster, D. J., Dobbs, F. C., Hammond, D., Hoover, D. J., Pope, R. H., *et al.* 1997. Latitudinal variations in benthic processes in the abyssal equatorial Pacific: control by biogenic particle flux. Deep Sea Research Part II: Topical Studies in Oceanography, 44: 2295–2317.

Smith, C. R., Paterson, G., Lambshead, J., Glover, A., Rogers, A., Gooday, A., Kitazato, H., *et al.* 2008a. Biodiversity, species ranges, and gene flow in the abyssal Pacific nodule province: predicting and managing the impacts of deep seabed mining. Monograph, ISA technical study, 3. International Seabed Authority. http://eprints.soton.ac.uk/63301/ (Accessed 3 July 2014).

Smith, C. R., De Leo, F. C., Bernardino, A. F., Sweetman, A. K., and Martinez Arbizu, P. 2008b. Abyssal food limitation, ecosystem structure and climate change. Trends in Ecology and Evolution, 23: 518–528.

Smith, K. L. Jr., Ruhl, H. A., Huffard, C. L., Messié, M., and Kahru, M. 2018. Episodic organic carbon fluxes from surface ocean to abyssal depths during long-term monitoring in NE Pacific. PNAS, 115: 12235–12240.

Sweetman, A. K., Smith, C. R., Shulse, C. N., Maillot, B., Lindh, M., Church, M. J., Meyer, K. S., *et al.* 2019. Key role of bacteria in the short-term cycling of carbon at the abyssal seafloor in a low particulate organic carbon flux region of the eastern Pacific Ocean. Limnology and Oceanography, 0. https://aslopubs.onlinelibrary.wiley.com/doi/abs/10.1002/lno.11069 (Accessed 6 December 2018).

Thiel, H., Schriever, G., Bussau, C., and Borowski, C. 1993. Manganese nodule crevice fauna. Deep Sea Research Part I: Oceanographic Research Papers, 40: 419–423.

Thistle, D., and Wilson, G. D. F. 1987. A hydrodynamically modified, abyssal isopod fauna. Deep Sea Research Part A. Oceanographic Research Papers, 34: 73–87.

Thistle, D., and Wilson, G. D. F. 1996. Is the HEBBLE isopod fauna hydrodynamically modified? A second test. Deep Sea Research Part I: Oceanographic Research Papers, 43: 545–554.

Vanreusel, A., Hilario, A., Ribeiro, P. A., Menot, L., and Arbizu, P. M. 2016. Threatened by mining, polymetallic nodules are required to preserve abyssal epifauna. Scientific Reports, 6: 26808.

Vavrek, M. J. 2020. fossil: Palaeoecological and Palaeogeographical Analysis Tools. https://CRAN.R-project.org/package=fossil.

Veillette, J., Sarrazin, J., Gooday, A. J., Galéron, J., Caprais, J.-C., Vangriesheim, A., Étoubleau, J., *et al.* 2007a. Ferromanganese nodule fauna in the Tropical North Pacific Ocean: Species richness, faunal cover and spatial distribution. Deep Sea Research Part I: Oceanographic Research Papers, 54: 1912–1935.

Veillette, J., Juniper, S. K., Gooday, A. J., and Sarrazin, J. 2007b. Influence of surface texture and microhabitat heterogeneity in structuring nodule faunal communities. Deep Sea Research Part I: Oceanographic Research Papers, 54: 1936–1943.

Volz, J. B., Mogollón, J. M., Geibert, W., Arbizu, P. M., Koschinsky, A., and Kasten, S. 2018. Natural spatial variability of depositional conditions, biogeochemical processes and element fluxes in sediments of the eastern Clarion-Clipperton Zone, Pacific Ocean. Deep Sea Research Part I: Oceanographic Research Papers, 140: 159–172.

Wiklund, H., Neal, L., Glover, A. G., Drennan, R., Rabone, M., and Dahlgren, T. G. 2019. Abyssal fauna of polymetallic nodule exploration areas, eastern Clarion-Clipperton Zone, central Pacific Ocean: Annelida: Capitellidae, Opheliidae, Scalibregmatidae, and Travisiidae. ZooKeys, 883: 1–82.

Wilson, G. D. F. 1987. Crustacean communities of the manganese nodule province (DOMES site A compared with DOMES site C). Report for the National Oceanic and Atmospheric Administration Of-

fice of the Ocean Coastal Resource Management (Ocean, Minerals and Energy). On Contract Na-84-Abh-0300: 40.

Wilson, G. D. F. 2008. Local and regional species diversity of benthic Isopoda (Crustacea) in the deep Gulf of Mexico. Deep-Sea Research II, 55: 2634–2649.

Wilson, G. D. F. 2017. Macrofauna abundance, species diversity and turnover at three sites in the Clipperton-Clarion Fracture Zone. Marine Biodiversity, 47: 323–347.

9 Figures

Figure 1. Map of the Clarion Clipperton Fracture Zone polymetallic nodule fields with represented in green the GSR contract area with the three sub-areas (B2, B4, B6) and a magnification of the sampling stations within the B4S03 site. Depth range: 4420 m (black) - 4591 m (white).

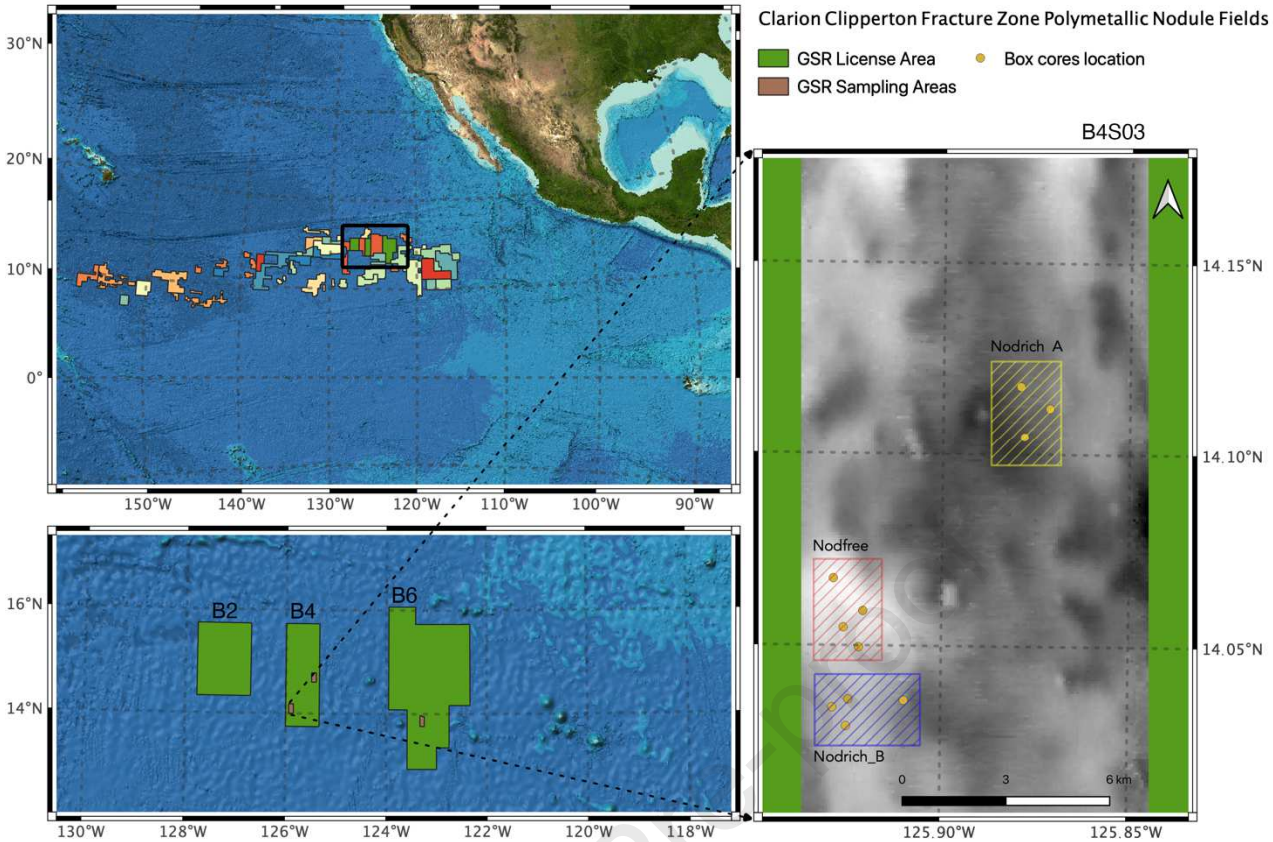

Figure 2. Principal component analysis (PCA) of the sediment environmental variables (including pigments) for the 0-5 cm layer for the three stations (Nodfree in red, Nodrich_A in yellow, Nodrich_B in blue), based on Euclidean distance similarities on the normalised data . The vectors represent the environmental variables and the two axes represent the two most important principal components (PC1 and PC2) and the percentage of variability they explain is reported. The ellipses represent the 0.95 confidence interval of the data distribution of each station around a centroid.

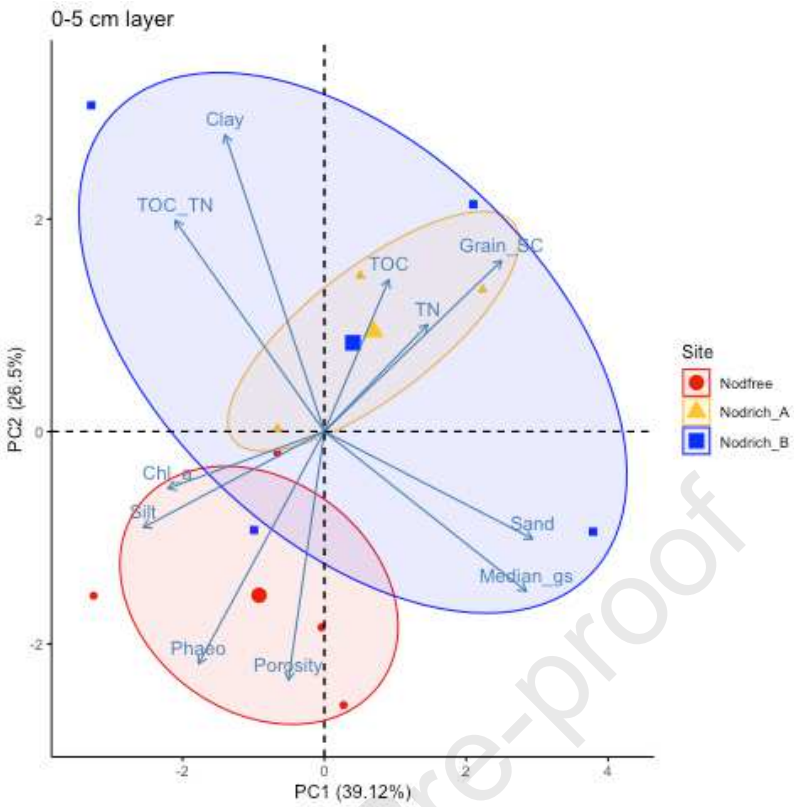

Figure 3. Monthly-averaged net primary production (NPP) in the B4S03 site for the period June 2015 - June 2017. The blue vertical band represents the timing of the previous GSRNOD15A cruise event (September-October 2015) whereas the orange vertical band refers to the present study GSRNOD17 sampling campaign of May-June 2017.

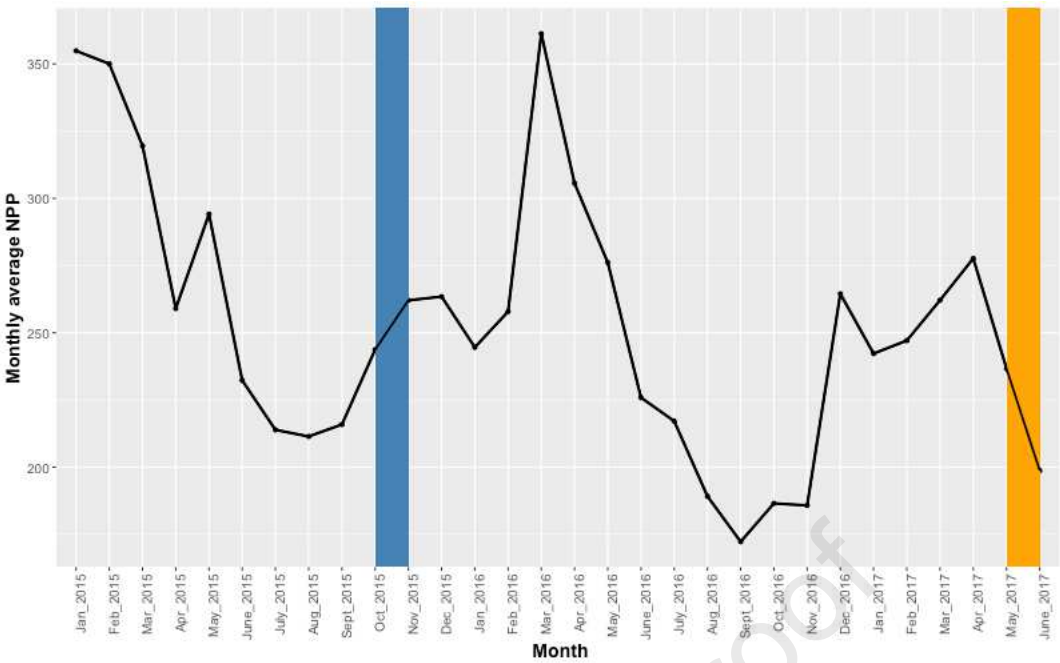

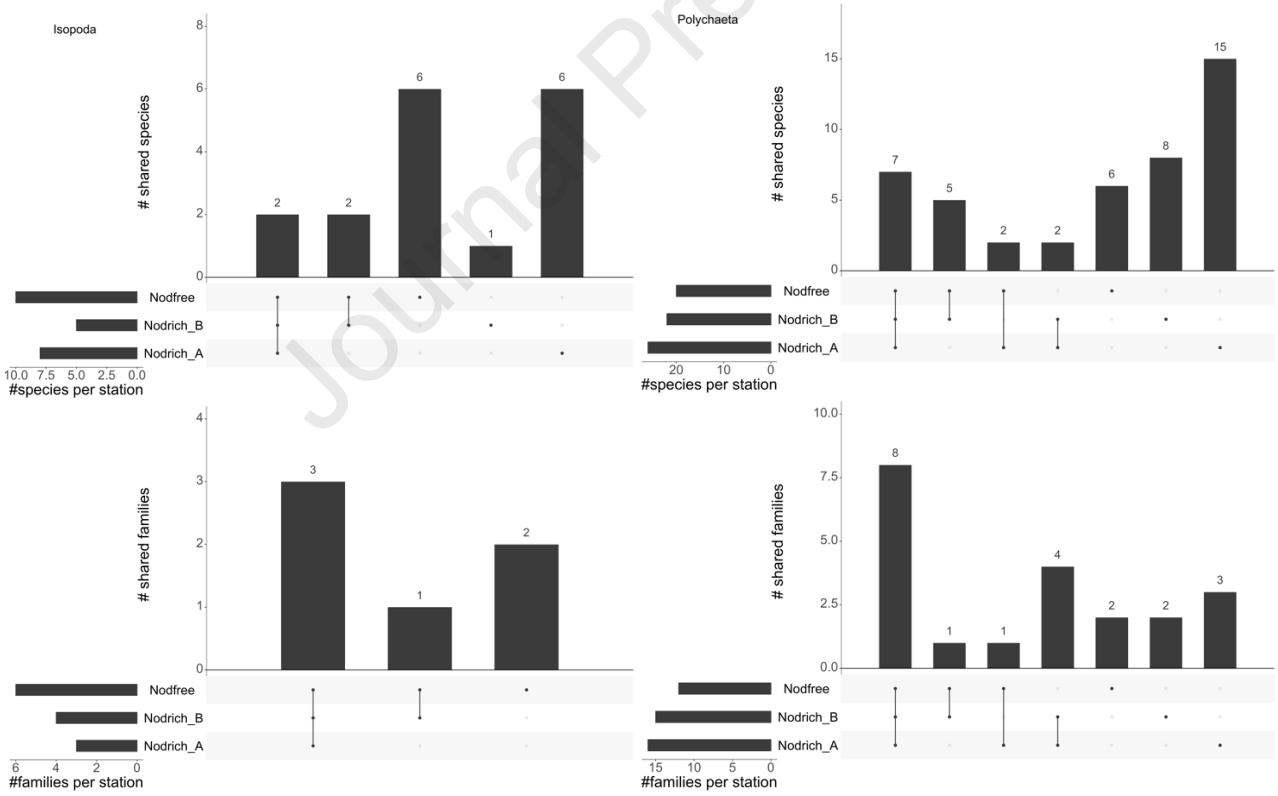

Figure 4 Upset matrix design bi-plots representing shared and unique species (upper plot) and families (lower plot) across the three stations per each of the dominant taxa (Isopoda, Polychaeta, Tanaidacea). Dots when united by a line represent the shared species/families between the different stations, for which the total number of species is reported on top of the bar. Single dots represent unique species per station.

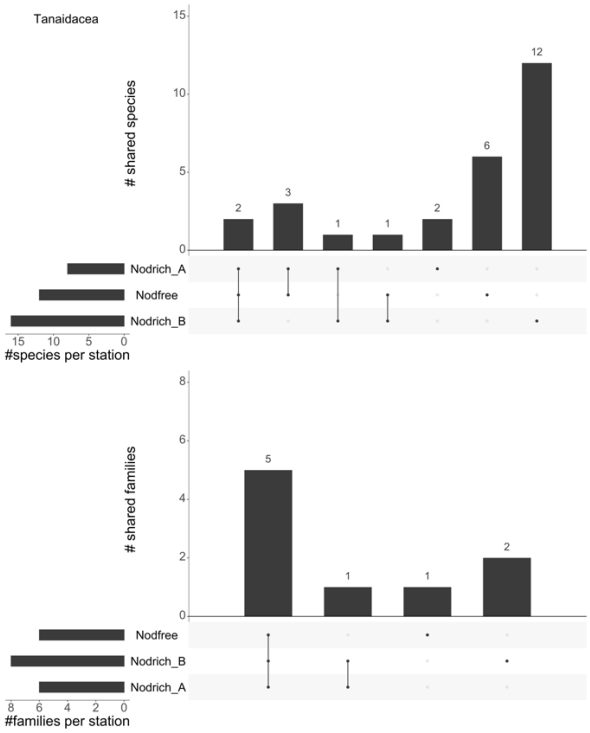

Figure 4 (continued) Upset matrix design bi-plots representing shared and unique species (upper plot) and families (lower plot) across the three stations per each of the dominant taxa (Isopoda, Polychaeta, Tanaidacea). Dots when united by a line represent the shared species/families between the different stations, for which the total number of species is reported on top of the bar. Single dots represent unique species per station.

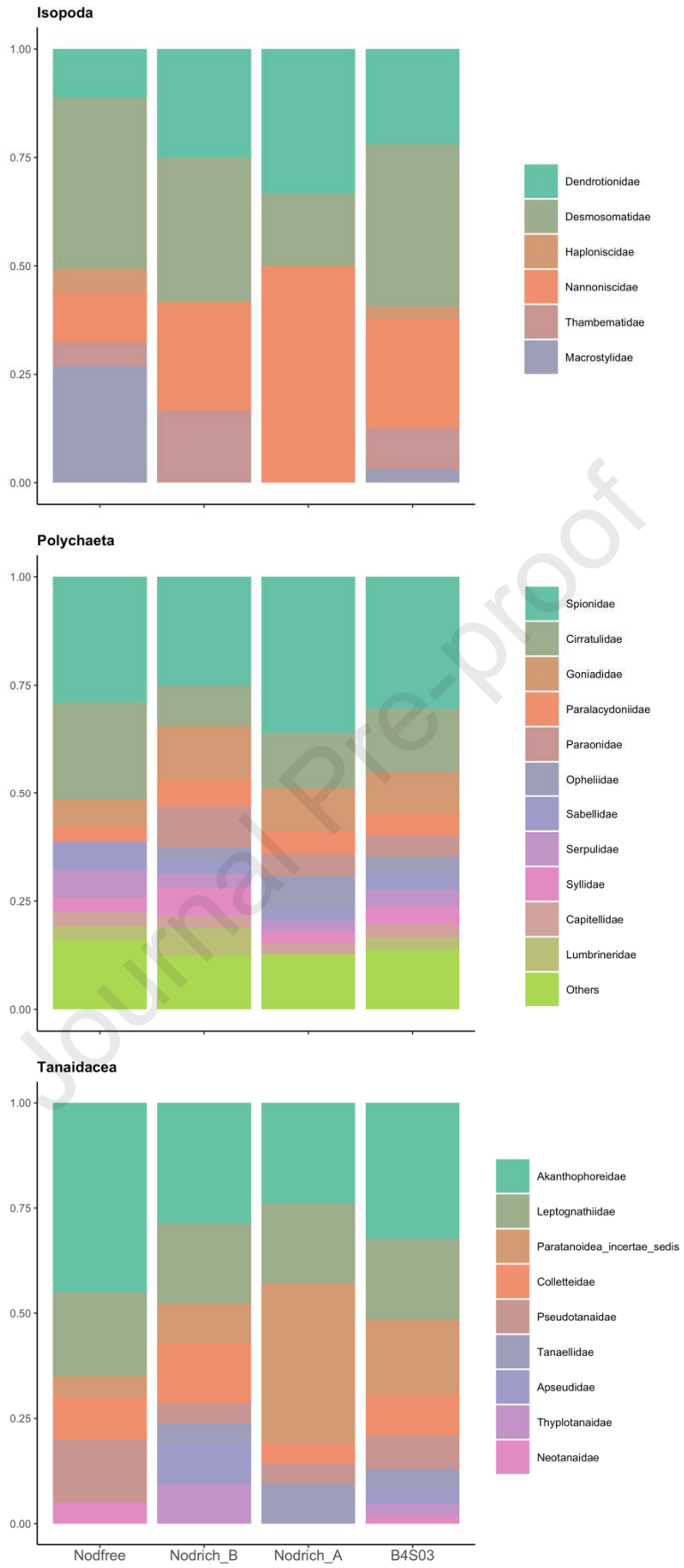

Figure 5. Family composition for the three dominant taxa (Polychaeta, Isopoda, Tanaidacea) displayed as average relative abundance per station and for the whole investigated site B4S03.

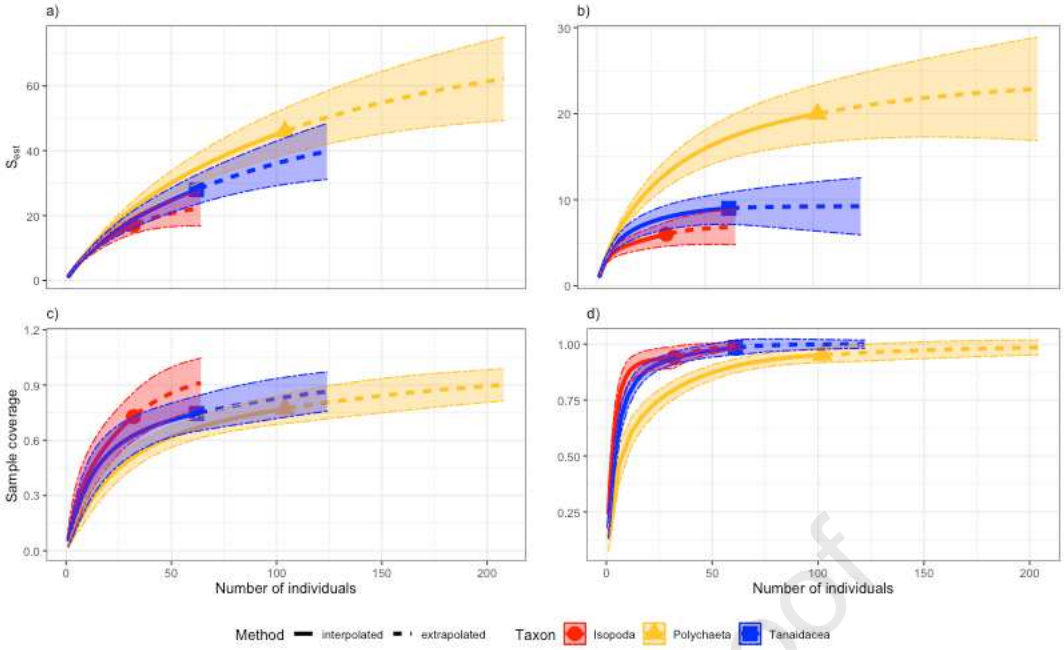

Figure 6. Sample-size-based and (a-b) coverage-based (c-d) rarefaction (solid line segment) and extrapolation (dotted line segments) sampling curves for species (species level = left side plots ; family level = right side plots) richness (Hill's number q = 0) with 95% confidence intervals (shaded areas) for each taxon (Isopoda in red, Polychaeta in yellow, Tanaidacea in blue) for site B4S03.

10 Tables

Table 1 a. Results of the multivariate/univariate two-way abiotic variables and one-way (b) biotic variables Permanova with Permdisp test results. Statistical significance is marked with a (*), NS indicate non statistically significant results.

Analysis	Parameter	Factor	dF	P-value	Permdisp
Abiotic variables					
Multivariate Two-way Permanova	Environmental variables (all)	Station	2	0.06 ·	-
		Layer	1	0.01 *	0.003 **
		Station*Layer	5	0.11	-
Univariate Two-way Permanova	TOC%	Station	2	NS	-
		Layer	1	0.04*	NS
		Station*Layer	2	NS	-
	TN%	Station	2	NS	-
		Layer	1	NS	-
		Station*Layer	2	NS	-
	TOC/TN	Station	2	NS	-
		Layer	1	0.07·	-
		Station*Layer	2	NS	-
	Porosity	Station	2	0.0015	NS
		Layer	1	0.0001**	NS
		Station*Layer	2	NS	-
	Median_gs	Station	2	NS	-
		Layer	1	NS	-
		Station*Layer	2	NS	-
	Grain_SC	Station	2	0.02*	NS
		Layer	1	NS	-
		Station*Layer	2	0.3	-
	Sand%	Station	2	NS	-
		Layer	1	NS	-
		Station*Layer	2	NS	-
	Silt%	Station	2	NS	-
		Layer	1	NS	-
		Station*Layer	2	NS	-
	Clay%	Station	2	0.039*	0.035*
		Layer	1	NS	-
		Station*Layer	2	NS	-
	Chl-a	Station	2	0.06 ·	-
		Layer	4	0.0067 **	-
		Station*Layer	8	0.0071 **	0.001 ***
	Phaeopigments	Station	2	0.03 *	-
		Layer	4	0.0001 *	-
		Station*Layer	8	0.0088 **	0.001 ***
	CPE	Station	2	0.03 *	-
		Layer	4	0.0001 *	-
		Station*Layer	8	0.0064 **	0.001 ***
Univariate One-way Permanova	Nodule abundance	Station	2	0.0042 **	NS
	Nodule coverage (%)	Station	2	0.04*	NS

Table 1 b. Results of the multivariate/univariate one-way Permanova on the biotic variables with Permdisp test results. Statistical significance is marked with a (*), NS indicate non statistically significant results.

Analysis	Parameter	Factor	dF	P-value	Permdisp
Higher Taxon macrofauna (excl.meiofauna)					
Univariate One-way Permanova	Total abundance	Station	2	NS	NS
Multivariate One-way Permanova	Taxon composition	Station	2	NS	NS
ISOPODA					
Higher Taxon (Family)					
Univariate One-way Permanova	Diversity indices:	Station	2		
	T (family richness)			NS	NS
	H' (Shannon-Wiener)			NS	NS
	J (Pileou's eveness)			NS	NS
	ES(4)			NS	NS
Multivariate One-way Permanova	Family composition	Station	2	NS	NS
Lower Taxon (Species)					
Univariate One-way Permanova	Diversity indices:	Station	2		
	S (species richness)			NS	NS
	H' (Shannon-Wiener)			NS	NS
	J (Pileou's eveness)			NS	NS
	ES(4)			NS	NS
Multivariate One-way Permanova	Species composition	Station	2	NS	NS
POLYCHAETA					
Higher Taxon (Family)					
Univariate One-way Permanova	Diversity indices:	Station	2		
	T (family richness)			NS	NS
	H' (Shannon-Wiener)			NS	0.003 **
	J (Pileou's eveness)			NS	0.001 ***
	ES(4)			NS	0.004 **
Multivariate One-way Permanova	Family composition	Station	2	NS	NS
Lower Taxon (Species)					
Univariate One-way Permanova	Diversity indices:	Station	2		
	S (species richness)			NS	NS
	H' (Shannon-Wiener)			NS	0.032 *
	J (Pileou's eveness)			NS	0.001 ***
	ES(4)			NS	0.001 ***
Multivariate One-way Permanova	Species composition	Station	2	NS	NS

Table 1 b (Continued). Results of the multivariate/univariate one-way Permanova on the biotic variables with Permdisp test results. Statistical significance is marked with a (*), NS indicate non statistically significant results.

Analysis	Parameter	Factor	dF	P-value	Permdisp
TANAIDACEA					
Higher Taxon (Family)					
Univariate One-way Permanova	Diversity indices:	Station	2		
	T (family richness)			NS	NS
	H' (Shannon-Wiener)			NS	NS
	J (Pileou's eveness)			0.07 ·	0.001 ***
	ES(4)			NS	NS
Multivariate One-way Permanova	Family composition	Station	2	NS	NS
Lower Taxon (Species)					
Univariate One-way Permanova	Diversity indices:	Station	2		
	T (species richness)			NS	NS
	H' (Shannon-Wiener)			NS	NS
	J (Pileou's eveness)			NS	0.001 ***
	ES(4)			NS	NS
Multivariate One-way Permanova	Species composition	Station	2	NS	0.001 ***

Table 2. Average values ± standard deviation of the environmental parameters: sand content (%), silt content (%), clay content (%), porosity (% vol), nodule abundance (Kg m-2), Chlorphyll-a (µg/g), Phaeopigments (µg/g), TOC= total organic carbon; TN = total nitrogen.

	Sand (%)		Silt (%)		Clay (%)		Porosity (% vol)		Median_gs	
	0-5 cm	5 -10 cm	0-5 cm	5 -10 cm	0-5 cm	5 -10 cm	0-5 cm	5 -10 cm	0-5 cm	5 -10 cm
Nodfree	9.15 ± 0.90	10.24 ± 0.60	74.38 ± 0.44	73.91 ± 0.29	16.45 ± 0.49	15.83 ± 0.34	0.893 ± 0.008	0.86 ± 0.007	16.95 ± 0.89	17.70 ± 0.93
Nodrich_B	9.38 ±2.51	8.79 ± 3.23	72.87 ± 1.64	74.04 ± 1.91	17.73 ± 1.29	17.15 ± 1.52	0.89 ± 0.005	0.84 ± 0.006	16.77 ± 2.09	16.55 ± 2.42
Nodrich_A	9.22 ± 0.96	6.52 ± 0.26	73.63 ± 0.99	75.27 ± 0.06	17.13 ± 0.16	18.19 ± 0.30	0.88 ± 0.007	0.83 ± 0.006	17.08 ± 0.57	15.61 ± 0.26

	Grain_SC		Chlorphyll-a (µg/g)		Phaeopigments (µg/g)		TOC (%)		TN (%)		Nodule abundance
	0-5 cm	5 -10 cm	0-5 cm	5 -10 cm	0-5 cm	5 -10 cm	0-5 cm	5 -10 cm	0-5 cm	5 -10 cm	Kg m-2
Nodfree	1.209 ± 0.013	1.210 ± 0.014	0.0012 ± 0.0014	NA	0.017 ± 0.01	NA	0.68 ± 0.01	0.62 ± 0.03	0.20 ± 0.01	0.22 ± 0.02	0.63 ± 0.72
Nodrich_B	1.267 ± 0.035	1.221 ± 0.035	0.000 ± 0.000	NA	0.0109 ± 0.0065	NA	0.59 ± 0.06	0.53 ± 0.11	0.29 ± 0.20	0.21 ± 0.06	20.01 ± 5.56
Nodrich_A	1.272 ± 0.031	1.248 ± 0.013	0.00038 ± 0.00052	NA	0.0073 ± 0.0072	NA	0.62 ± 0.03	0.54 ± 0.04	0.21 ± 0.00	0.19 ± 0.01	24.17 ± 1.54

Table 3. Diversity indices of the three main taxa at the family and species level . T= taxon richness (species or family); H' = Shannon Wiener diversity index; J' = Pilou's evenness index; rarefaction method of Sanders for expected species ES(4). Values are reported as average ± standard deviation.

ISOPODA	T	H'	J'	ES(4)
Family level				
Nodfree	3.33 ± 1.52	1.04 ± 0.45	0.91 ± 0.11	2.35 ± 0.56
Nodrich_B	2.25 ± 1.25	0.68 ± 0.55	0.99 ± 0.01	1.92 ± 0.72
Nodrich_A	1.66 ± 0.57	0.44 ± 0.38	0.95 ± 0.05	1.60 ± 0.53
Species level				
Nodfree	3.66 ± 0.15	1.16 ± 0.43	0.95 ± 0.05	2.52 ± 0.51
Nodrich_B	2.50 ± 0.17	0.73 ± 0.63	0.74 ± 0.49	1.97 ± 0.80
Nodrich_A	2.00 ± 0.01	0.59 ± 0.55	0.66 ± 0.57	1.84 ± 0.79
POLYCHAETA	T	H'	J'	ES(4)
Family level				
Nodfree	4.5 ± 2.73	1.24 ± 0.76	0.97 ± 0.02	2.55 ± 0.90
Nodrich_B	1.62 ± 1.06	0.33 ± 051	0.97 ± 0.04	1.46 ± 0.71
Nodrich_A	4.0 ± 2.52	1.21 ± 0.46	0.97 ± 0.03	2.59 ± 0.44
Species level				
Nodfree	9.0 ± 1.73	2.15 ± 0.17	0.98 ± 0.01	3.43 ± 0.09
Nodrich_B	6.75 ± 4.92	1.53 ± 1.06	0.73 ± 0.48	2.75 ± 1.17
Nodrich_A	10.6 ± 1.15	2.29 ± 0.07	0.97 ± 0.02	3.48 ± 0.06
TANAIDACEA	T	H'	J'	ES(4)
Family level				
Nodfree	3.33 ± 1.15	1.07 ± 0.33	0.94 ± 0.06	2.38 ± 0.40
Nodrich_B	3.50 ± 1.29	1.14 ± 0.36	0.96 ± 0.02	2.50 ± 0.41
Nodrich_A	3.66 ± 2.30	0.92 ± 0.80	0.86 ± 0.07	2.11 ± 0.98
Species level				
Nodfree	5.66 ± 2.5	1.61 ± 0.52	0.97 ± 0.02	2.99 ± 0.52
Nodrich_B	4.50 ± 1.91	1.40 ± 0.50	0.99 ± 0.01	2.81 ± 0.58
Nodrich_A	4.0 ± 2.64	1.01 ± 0.90	0.59 ± 0.52	2.22 ± 1.11
ALL THREE TAXA (Species)	T	H'	J'	ES(4)
Nodfree	18.33 ± 2.51	2.85 ± 0.144	0.32 ± 0.01	4.84 ± 0.086
Nodrich_B	13.75 ± 6.50	2.46 ± 0.59	0.37 ± 0.08	4.88 ± 0.09
Nodrich_A	16.66 ± 2.08	2.65 ± 0.19	0.32 ± 0.01	4.58 ± 0.23

Table 4. B4S03 site lower-taxon (species) non-parametric diversity estimation analysis. S_{obs} = observed species diversity; S_{Chao1} = Chao1 asymptotic estimated diversity; S_{obs}/S_{Chao1}= recorded diversity based on Chao1 estimator. The second part of the Table ("Necessary sampling effort") reports the results of the calculations

based on the S_{Chao1} asymptotic diversity of how many extra samples/individuals/area should be sampled to record a diversity g = x (e.g. as fraction of the asymptotic estimated diversity S_{Chao1}).

	Isopoda	Polychaeta	Tanaidacea
n° samples taken	10	10	10
n° of singletons	9	24	16
n° of doubletons	5	10	5
n (individuals identified)	31	104	62
S_{obs}	17	46	28
S_{Chao1} (non-parametric estimator)	25	74.8	53.6
Recorded diversity (S_{obs} / S_{Chao1})	0.68	0.61	0.52
Necessary sampling effort (Chao et al., 2014)			
g=1			
Additional individuals	126	745	575
Additional samples	41	72	93
Tot. samples needed	51	82	103
Times original sample size	5	8	10
Total area (m^2) to be samples to reach g	13	20	26
g must be greater than	0.77	0.77	0.47
g = 0.95			
Additional individuals	33	336	155
Additional samples	11	32	25
Tot. samples needed	21	42	35
Times original sample size	2	4	4
Total area (m^2) to be samples to reach g	5	11	9
g=0.80			
Additional individuals	13	163	86
Additional samples	4	16	14
Total samples needed	14	26	24
Times original sample size	1	3	2
Total area (m^2) to be samples to reach g	4	6	6

11 Supplementary material: Figures and Tables

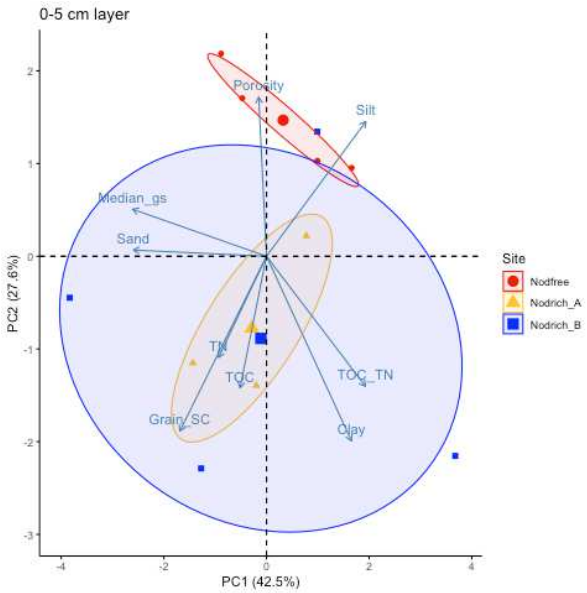

SF1. Principal component analysis (PCA) of the sediment environmental variables (excl. pigments and nodule abundance) for the 0-5 cm layer for the three stations (Nodfree in red, Nodrich_A in yellow, Nodrich_B in

blue), based on Euclidean distance similarities on the normalised data. The vectors represent the environmental variables and the two axes represent the two most important principal components (PC1 and PC2) and the percentage of variability they explain is reported. The ellipses represent the 0.95 confidence interval of the data distribution of each station around a centroid.

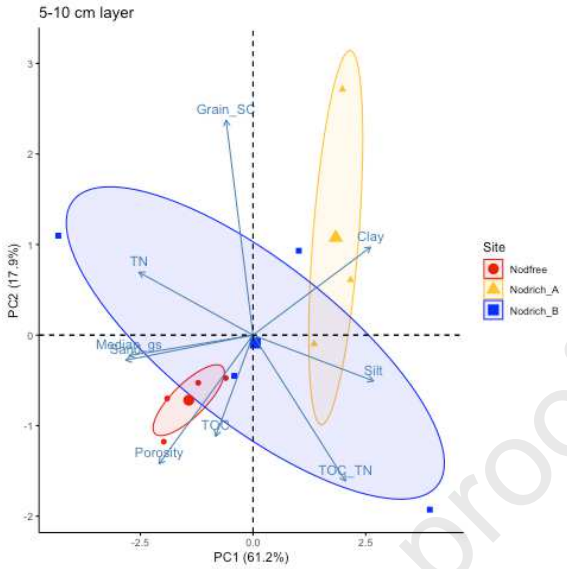

SF2. Principal component analysis (PCA) of the sediment environmental variables (excl. pigments and nodule abundance) for the 5-10 cm layer for the three stations (Nodfree in red, Nodrich_A in yellow, Nodrich_B in blue), based on Euclidean distance similarities on the normalised data. The vectors represent the environmental variables and the two axes represent the two most important principal components (PC1 and PC2) and the percentage of variability they explain is reported. The ellipses represent the 0.95 confidence interval of the data distribution of each station around a centroid.

Supplementary Table ST1. Details of multicorer (MUC) and boxcorer (BC) samples collected during GSRNOD17 cruise. Deployments dates are the date at which the deployment touched the floor. Coordinates are those of the MUC/BC touchdown.

	SampleID	Station ID	Date	Latitude (N)	Longitude (W)	Deployment depth (m)	Analysis
Multicorer							
	MUC011	Nodfree	26/05/2017	14° 04' 0.088"	125° 55' 44.437"	4649	
	MUC012	Nodfree	26/05/2017	14° 03' 33.74998"	125° 55' 15.19011"	4575	
	MUC013	Nodfree	27/05/2017	14° 03' 14.05729"	125° 55' 26.86686"	4573	
	MUC020	Nodfree	01/06/2017	14° 02' 59.48021"	125° 55' 17.74194"	4557	
	MUC014	Nodrich_B	28/05/2017	14° 02' 10.71719"	125° 55' 28.34904"	4537	
	MUC015	Nodrich_B	28/05/2017	14° 01' 45.23694"	125° 55' 30.26248"	4555	Biogeochemistry
	MUC016	Nodrich_B	28/05/2017	14° 02' 00.95803"	125° 55' 44.49076"	4545	
	MUC021	Nodrich_B	03/06/2017	14° 02' 08.20105"	125° 54' 35.65350"	4550	
	MUC017	Nodrich_A	30/05/2017	14° 06' 14.91210"	125° 52' 42.06784"	4480	
	MUC018	Nodrich_A	30/05/2017	14° 06' 43.72101"	125° 52' 17.59307"	4510	
	MUC019	Nodrich_A	30/05/2017	14° 07' 03.34491"	125° 52' 46.14806"	4500	
Box-corer							
	BC037	Nodfree	26/05/2017	14° 04' 02.81202"	125° 55' 44.40113"	4629	
	BC039	Nodfree	27/05/2017	14° 03' 32.45348"	125° 55' 15.66124"	4585	
	BC056	Nodfree	02/06/2017	14° 02' 58.49970"	125°55' 19.39387"	4558	
	BC042	Nodrich_B	28/05/2017	14° 02' 09.47831"	125° 55' 29.03077"	4552	Macrofauna higher/ lower taxon analysis - Nodule abundance estimation
	BC043	Nodrich_B	28/05/2017	14° 02' 01.97395"	125° 55' 44.46696"	4546	
	BC045	Nodrich_B	28/05/2017	14° 01' 44.57942"	125° 55' 31.03251"	4554	
	BC057	Nodrich_B	03/06/2017	14° 02' 08.90255"	125° 54' 35.57861"	4509	
	BC050	Nodrich_A	29/05/2017	14° 06' 16.67737"	125° 52' 41.48177"	4481	
	BC053	Nodrich_A	30/05/2017	14° 10' 16.59182"	125° 55' 01.98463"	4588	
	BC054	Nodrich_A	31/05/2017	14° 07' 04.34218"	125° 52' 45.41828"	4502	

ST2. Higher-taxon densities expressed as individuals m^{-2} for macrofauna and meiofauna (total counts multiplied by a factor 4) per each box-core per station during GSRNOD17.

	Nodfree			Nodrich_B				Nodrich_A		
	BC037	BC039	BC056	BC042	BC043	BC045	BC057	BC052	BC054	BC050
Macrofauna Taxa										
Amphipoda	0	0	4	4	0	36	12	4	16	0
Bivalvia	4	8	8	0	4	8	12	8	12	4
Chaetognata	0	0	0	0	0	4	0	4	0	0
Gastropoda	0	0	0	0	0	4	0	0	4	0
Isopoda	48	28	20	12	12	8	28	16	8	12
Oligochaeta	0	0	0	0	0	0	0	4	0	0
Ophiuroidea	0	4	0	0	4	0	0	0	0	0
Polychaeta	60	88	132	128	20	60	96	128	96	116
Scaphopoda	0	0	0	0	0	0	4	0	0	0
Tanaidacea	20	44	40	48	8	16	28	4	60	12
Unknown	8	4	8	0	16	16	0	4	16	8
	0	0	0	0	0	0	0	0	0	0
Total abundance	140	176	212	192	64	152	180	172	212	152
Meiofauna Taxa										
Copepoda	60	100	144	64	12	28	72	80	56	36
Nematoda	4	44	72	48	0	12	32	28	32	8
Ostracoda	0	20	16	24	0	20	32	12	32	8
Foraminifera	0	0	4	4	0	0	8	0	0	4
Euphasiacea	0	0	0	0	4	0	0	0	0	0
Total abundance	64	164	236	140	16	60	144	120	120	56

ST3 a Permdisp analysis results and pair-wise tests for abiotic variables.

Analysis	Parameter	Factor	Permdisp	Pair-wise test		
Abiotic variables						
Multivariate Two-way Permanova	Environmental variables (all)	Station	-	–	–	–
		Layer	0.003 **	0-5 cm layer differ from 5-10 cm layer		
		Station*Layer	-	–	–	–
Univariate Two-way Permanova	TOC%	Station	-	–	–	–
		Layer	NS	0-5 cm differs from 5-10 cm p = 0.008*		
		Station*Layer	-	–	–	–
	TN%	Station	-	–	–	–
		Layer	-	–	–	–
		Station*Layer	-	–	–	–
	TOC/TN	Station	-	–	–	–
		Layer	-	–	–	–
		Station*Layer	-	–	–	–
	Porosity	Station	NS	Nodfree-Nodrich_B NS	Nodfree-Nodrich_A NS	Nodrich_A-Nodrich_B NS
		Layer	NS	0-5 cm differs from 5-10 cm p=0.0001***		
		Station*Layer	-	–	–	–
	Median_gs	Station	-	–	–	–
		Layer	-	–	–	–
		Station*Layer	-	–	–	–
	Grain_SC	Station	NS	Nodfree-Nodrich_B NS	Nodfree-Nodrich_A 0.0009 ***	Nodrich_A-Nodrich_B NS
		Layer	-	–	–	–
		Station*Layer	-	–	–	–
	Sand%	Station	-	–	–	–
		Layer	-	–	–	–
		Station*Layer	-	–	–	–
	Silt%	Station	-	–	–	–
		Layer	-	–	–	–
		Station*Layer	-	–	–	–
	Clay%	Station	0.035*	–	–	–
		Layer	-	–	–	–
		Station*Layer	-	–	–	–
	Chl-a	Station	-	–	–	–
		Layer	-	–	–	–
		Station*Layer	0.001 ***	---------- NS ----------		
	Phaeopigments	Station	-	–	–	–
		Layer	-	–	–	–
		Station*Layer	0.001 ***	All depth layers differ from one another only within Nodfree		
	CPE	Station	-	–	–	–
		Layer	-	–	–	–
		Station*Layer	0.001 ***	All depth layers differ within Nodfree / Nodrich_A and Nodrich_B deeper layers (excl. 0-1 cm) all differ from the deeper layers of Nodfree		
Univariate One-way Permanova	Nodule abundance	Station	NS	Nodfree-Nodrich_B 0.0007 **	Nodfree-Nodrich_A 0.00035 **	Nodrich_A-Nodrich_B NS
	Nodule coverage (%)	Station	NS	Nodfree-Nodrich_B 0.08*	Nodfree-Nodrich_A 0.05*	Nodrich_A-Nodrich_B NS

ST3 b Permdisp analysis results and pair-wise tests for biotic variables.

Analysis	Parameter	Factor	Permdisp	Pair-wise test		
Higher Taxon macrofauna (excl.meiofauna)						
Univariate One-way Permanova	Total abundance	Station	NS	–	–	–
Multivariate One-way Permanova	Taxon composition	Station	NS	–	–	–
ISOPODA						
Higher Taxon (Family)						
Univariate One-way Permanova	Diversity indices:	Station				
	T (family richness)		NS	–	–	–
	H' (Shannon-Wiener)		NS	–	–	–
	J (Pileou's eveness)		NS	–	–	–
	ES(4)		NS	–	–	–
Multivariate One-way Permanova	Family composition	Station	NS	–	–	–
Lower Taxon (Species)						
Univariate One-way Permanova	Diversity indices:	Station				
	S (species richness)		NS	–	–	–
	H' (Shannon-Wiener)		NS	–	–	–
	J (Pileou's eveness)		NS	–	–	–
	ES(4)		NS	–	–	–
Multivariate One-way Permanova	Species composition	Station	NS	–	–	–
POLYCHAETA						
Higher Taxon (Family)						
Univariate One-way Permanova	Diversity indices:	Station				
	T (family richness)		NS	–	–	–
	H' (Shannon-Wiener)		0.003 **	–	–	–
	J (Pileou's eveness)		0.001 ***	–	–	–
	ES(4)		0.004 **	–	–	–
Multivariate One-way Permanova	Family composition	Station	NS	–	–	–
Lower Taxon (Species)						
Univariate One-way Permanova	Diversity indices:	Station				
	S (species richness)		NS	–	–	–
	H' (Shannon-Wiener)		0.032 *	–	–	–
	J (Pileou's eveness)		0.001 ***	–	–	–
	ES(4)		0.001 ***	–	–	–
Multivariate One-way Permanova	Species composition	Station	NS	–	–	–
TANAIDACEA						
Higher Taxon (Family)						
Univariate One-way Permanova	Diversity indices:	Station				
	T (family richness)		NS	–	–	–
	H' (Shannon-Wiener)		NS	–	–	–
	J (Pileou's eveness)		0.001 ***	–	–	–
	ES(4)		NS	–	–	–
Multivariate One-way Permanova	Family composition	Station	NS	–	–	–
Lower Taxon (Species)						
Univariate One-way Permanova	Diversity indices:	Station				
	T (species richness)		NS	–	–	–
	H' (Shannon-Wiener)		NS	–	–	–
	J (Pileou's eveness)		0.001 ***	–	–	–
	ES(4)		NS	–	–	–
Multivariate One-way Permanova	Species composition	Station	0.001 ***	–	–	–

ST4. List of shared (between two or three sites) and unique (per station) species/morphospecies per each of the three main taxa. The (*) indicate that the species/morphospecies is a singleton (encountered only once

across samples). The "#number" refers to the specimen identifier. The specification (*cf*) means that the identification was done on a difficult to identify specimen (e.g. badly preserved or damaged).

	Shared species		Unique species		
TAXON	**Between all three sites**	**Between two sites**	**Nodfree**	**Nodrich_B**	**Nodrich_A**
ISOPODA					
	Dendrotion species A	*Chelator species B*	*Austroniscus* species (*)	*Desmosomatinae* species (*)	*Nannoniscus* species A (*)
	Thambema species A		*Chelator* species A	*Nannoniscus species C (*)*	*Nannoniscus* species B (*)
			Eugerdella species A		*Nannoniscus* species C
			Haploniscus species A (*)		*Panetela* species B
			Macrostylis metallicola (*)		*Prochelator* species A
			Mirabilicoxa species (*)		*Whoia* species A (*)
POLYCHAETA					
	Aphelochaeta species #1461	*Anguillosyllis* species *#1992*	*Aphelochaeta* species #1784	*Ammotrypanella* species (*)	*Serpulidae* species #1693 (*)
	Aphelochaeta species #1644	Capitellidae species #1821	*Chaetozone* species #1950	*Pseudoscalibregma (cf)* (*)	*Anguillosyllis* species #1990 (*)
	Aurospio dibranchiata #1457	*Ceratocephale (cf) abyssorum*	*Lacydonia* species #1412	*Goniadidae* species (*)	*Aphelochaeta* species #1644 (*)
	Aurospio dibranchiata #249	*Laonice* species	*Polaruchakov* species (*)	*Maldanidae* species #1915 (*)	*Aricidea* species #1911 (*)
	Bathyglycinde (cf)	*Lumbrinerides laubieri #2107*	*Prionospio* species #1426 (*)	*Paradoneis* species #1819 (*)	*Capitellidae* species #1718 (*)
	Paralacydonia paradoxa	Sabellidae species #1428	Serpulidae species #1429	*Parexogone* species (*)	*Dorvilleidae* species (*)
	Prionospio species #268	Sabellidae species #1756		*Poeciolochaetidae* species (*)	*Eulalia* species (*)
				Pseudomystides species (*)	*Glycera* species (*)
				Serpulidae species #1455 (*)	*Maldanidae* species #1742 (*)
					Octomagelona species (*)
					Opheliidae species *#1755* (*)
					Ophelina species #1706
					Paradoneis species #1737 (*)
					Prionospio species #1735
					Progoniada (cf) species (*)
TANAIDACEA					
	Forcipatia species #6	*Arthrura species #153*	*Neotanais species* #161 (*)	*Leptognathia* species (*)	*Collettea longisetosa* (*)
	Stenotanais species #59	*Caudalonga* species *#74*	New genus 4 species #162 (*)	*Leptognathiella occidentalis* (*)	*Tanabnormia species* #25 (*)
		Insociabilitanais species *#160*	*Parakanthophoreus* species #63 (*)	*Leptognathioides* species #18 (*)	
		Pseudotanais species *#158*	*Parakanthophoreus* species #95	*Leviapseudes* species #165 (*)	
		Tumidochelia species *#157*	*Pseudotanais geralti*	*Leviapseudes* species #166 (*)	
			Stenotanais species #55	New genus 1 species #152 (*)	
				New genus 2 species #151 (*)	
				New genus 3 species #156 (*)	
				New genus 5 species #20 (*)	
				Parakanthophoreus species #16A	
				Portarathrum species #155	
				Pseudotanais species #159 (*)	
				Stenotanais (cf.) species #164 (*)	

ST5. Main taxa families relative abundance (expressed as average % value) per station and across all samples (B4S03).

	Nodfree	Nodrich_B	Nodrich_A	B4S03
Isopoda				
Dendrotionidae	0.11	0.25	0.33	0.22
Desmosomatidae	0.39	0.33	0.17	0.38
Haploniscidae	0.06	0.00	0.00	0.03
Nannoniscidae	0.11	0.25	0.50	0.25
Thambematidae	0.06	0.17	0.00	0.09
Macrostylidae	0.27	0.00	0.00	0.03
Polychaeta				
Spionidae	0.29	0.25	0.36	0.30
Cirratulidae	0.23	0.09	0.13	0.15
Goniadidae	0.06	0.13	0.10	0.10
Paralacydoniidae	0.03	0.06	0.05	0.05
Paraonidae	0.00	0.09	0.05	0.05
Opheliidae	0.00	0.03	0.08	0.04
Sabellidae	0.06	0.03	0.03	0.04
Serpulidae	0.06	0.03	0.03	0.04
Syllidae	0.03	0.06	0.03	0.04
Capitellidae	0.03	0.03	0.03	0.03
Lumbrineridae	0.03	0.06	0.00	0.03
Nereididae	0.06	0.00	0.03	0.03
Lacydoniidae	0.06	0.00	0.00	0.02
Maldanidae	0.00	0.03	0.03	0.02
Phyllodocidae	0.00	0.03	0.03	0.02
Dorvilleidae	0.00	0.00	0.03	0.01
Magelonidae	0.00	0.00	0.03	0.01
Poeciolochaetidae	0.00	0.03	0.00	0.01
Polynoidae	0.03	0.00	0.00	0.01
Scalibregmatidae	0.00	0.03	0.00	0.01
Tanaidacea				
Akanthophoreidae	0.45	0.29	0.24	0.32
Leptognathiidae	0.20	0.19	0.19	0.19
Paratanoidea_incertae_sedis	0.05	0.10	0.38	0.18
Colletteidae	0.10	0.14	0.05	0.10
Pseudotanaidae	0.15	0.05	0.05	0.08
Tanaellidae	0.00	0.05	0.10	0.05
Apseudidae	0.00	0.10	0.00	0.03
Thyplotanaidae	0.00	0.10	0.00	0.03
Neotanaidae	0.05	0.00	0.00	0.02

Highlights

- GSR B4S03 nodule-rich and nodule-free stations are characterized by similar sedimentary parameters (sediment grain size, pigment content, TOC%)
- GSR B4S03 macrofauna of nodule-rich stations displayed comparable densities and higher-taxon diversity to that of nodule-free sediments
- For the dominant taxa (Polychaeta, Isopoda, Tanaidacea) the current sampling effort was insufficient to characterize the GSR B4S03 site diversity at morphospecies level but covered >90% of the diversity at the family level
- The high number of singletons, the patchiness and low densities of the dominant taxa may point to under-sampling bias with the risk to underestimate species diversity and overestimate endemism

Declaration of interests

☒ The authors declare that they have no known competing financial interests or personal relationships that could have appeared to influence the work reported in this paper.

☐The authors declare the following financial interests/personal relationships which may be considered as potential competing interests: